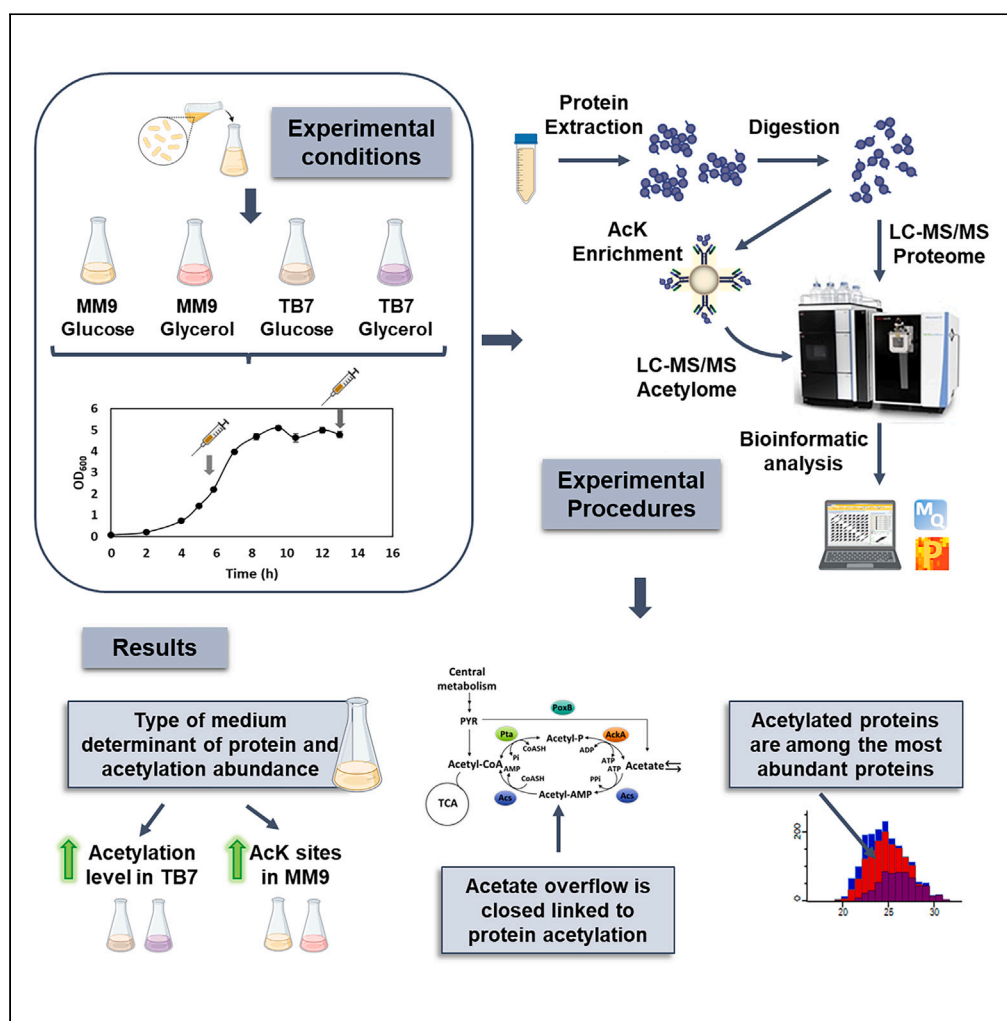**Article**

Relative impact of three growth conditions on the *Escherichia coli* protein acetylome

Gema Lozano-Terol, Riccardo Zenezini Chiozzi, Julia Gallego-Jara, ..., Albert J.R. Heck, Manuel Cánovas Díaz, Teresa de Diego Puente

tdp@um.es

Highlights

The type of medium is the main determinant of protein abundance and acetylation

Acetylation level is higher in complex media than in defined media

Acetylated proteins are among the most abundant proteins in all samples

Acetylation level and acetate overflow are closely linked

Article

Relative impact of three growth conditions on the *Escherichia coli* protein acetylome

Gema Lozano-Terol,[1] Riccardo Zenezini Chiozzi,[2,3] Julia Gallego-Jara,[1] Rosa Alba Sola-Martínez,[1] Adrián Martínez Vivancos,[1] Álvaro Ortega,[1] Albert J.R. Heck,[2] Manuel Cánovas Díaz,[1] and Teresa de Diego Puente[1,4,*]

SUMMARY

Nε-lysine acetylation is a common posttranslational modification observed in *Escherichia coli*. In the present study, integrative analysis of the proteome and acetylome was performed using label-free quantitative mass spectrometry to analyze the relative influence of three factors affecting growth. The results revealed differences in the proteome, mainly owing to the type of culture medium used (defined or complex). In the acetylome, 7482 unique acetylation sites were identified. Acetylation is directly related to the abundance of proteins, and the level of acetylation in each type of culture is associated with extracellular acetate concentration. Furthermore, most acetylated lysines in the exponential phase remained in the stationary phase without dynamic turnover. Interestingly, unique acetylation sites were detected in proteins whose presence or abundance was linked to the type of culture medium. Finally, the biological function of the acetylation changes was demonstrated for three central metabolic proteins (GapA, Mdh, and AceA).

INTRODUCTION

Escherichia coli is widely used in the production of a multitude of bioproducts and as a model organism because of the extensive knowledge of its genome, transcriptome, and proteome.[1] However, it is important to deepen our understanding of the processes regulating lysine acetylation that affect central metabolism. Proteome and post-translational modification (PTM) analyses provide a wide range of information on gene expression profiles and protein regulatory functions under certain conditions. Advances in liquid chromatography-mass coupled to mass spectrometry (LC-MS/MS) have provided further knowledge in this field.[2]

PTMs are essential for the regulation of cellular machinery as they allow modification of the activity, localization, or interaction of proteins, increasing functional proteomic variability.[3] Among these modifications, Nε-lysine acetylation plays an essential role in regulating different biological processes (BPs) and is highly conserved in all domains of life. This modification has been extensively studied in eukaryotes and has become increasingly relevant in prokaryotes in recent years.[4,5] Thus, it has recently been shown that up to 40% of proteins can be acetylated in bacteria.[4,6] Nε-lysine acetylation occurs through the transfer of an acetyl group from a donor, which can be acetyl-CoA or acetyl-P, to the ε-amino group of lysine side chain.[7] This modification is involved in the regulation of several cellular functions, including transcription, DNA damage repair, autophagy, metabolism, virulence factors, protein stability, protein-protein interactions or protein localization.[8,9] Lysine acetylation can occur enzymatically or non-enzymatically.[5,8] Enzymatic lysine acetylation is mediated by lysine acetyltransferases (KATs) by transferring the acetyl group from acetyl-CoA to the amino group of lysine. Non-enzymatical or chemical lysine acetylation occurs without the concurrence of enzymes, by transferring the acetyl group, mainly from acetyl-P, to lysine ε-amino group.[10–12] This type of acetylation also occurs in eukaryotes, especially mitochondria, using an acetyl-CoA acetyl donor.[13] Furthermore, Nε-lysine acetylation is a reversible modification that can be removed by the action of deacetylases. There are several types of deacetylases, including sirtuins. Sirtuins employ NAD^+ as a cosubstrate and transfer an acetyl group from lysine to the ribose of NAD^+. These enzymes are widely distributed across all life.[14] Sirtuin CobB is the only known and characterized in *E. coli*.[14,15]

In recent years, it has been shown that chemical acetylation contributes to the overall acetylation level of *E. coli*.[10,16] For non-enzymatic acetylation to take place, the deprotonation of lysine occurs first, and subsequently, the activated lysine incorporates the acetyl group of

[1]Department of Biochemistry and Molecular Biology and Immunology (B), Faculty of Chemistry, University of Murcia, Campus of Espinardo, Regional Campus of International Excellence "Campus Mare Nostrum", 30100 Murcia, Spain
[2]Biomolecular Mass Spectrometry and Proteomics, Bijvoet Centre for Biomolecular Research and Utrecht Institute for Pharmaceutical Sciences, Utrecht University, Padualaan 8, Utrecht 3584 CH, the Netherlands
[3]Present address: Mass-Spectrometry, Science Technology Platforms and Division of Biosciences, University College London, London, United Kingdom
[4]Lead contact
*Correspondence: tdp@um.es
https://doi.org/10.1016/j.isci.2024.109017

the donor through a nucleophilic attack.[10,12] Therefore, this type of acetylation depends on lysine reactivity and acetyl donor concentration. Lysine reactivity is determined by its pKa, microenvironment, and accessibility to a three-dimensional structure.[4,10] The concentration of acetyl donors is related to the acetate overflow.[17–20] Acetate overflow refers to the excretion, subsequent re-incorporation, and metabolism of this compound, which depends on the culture conditions employed.[20] In addition, the culture medium used (type of medium and carbon source) determines a higher or lower flux through glycolysis, affecting acetate overflow and, consequently acetyl donor concentration.[10,17–19,21] *E. coli* can consume different carbon sources, but preferentially uses those transported by the phosphoenolpyruvate phosphotransferase transport (PTS) system. However, the utilization of other carbon sources, such as glycerol (a non-PTS carbon source), is of significant interest because it is a by-product of biodiesel synthesis and represents an efficient use of resources.[22] With regard to the type of culture media, *E. coli* can be grown using rich or defined media. Rich media contain peptides that act as carbon and nitrogen sources and are usually used when the overall cell yield needs to be increased. However, the defined media must be supplemented with a carbon source, and be provided with inorganic ammonium as a source of nitrogen.[23] *E. coli* preferentially consumes inorganic ammonium, although it can use organic nitrogen sources such as amino acids.[24,25] The use of a rich or defined culture medium results in variations in the growth and differential expression of important proteins.[23] Therefore, central carbon metabolism is reorganized in response to the type of culture media.[23,26]

Numerous studies have been conducted on lysine acetylation in bacteria and its dynamics in relation to growth conditions,[17,27–33] considering individual factors. In this context, we set out to study the influence of the three growth factors simultaneously to determine their relative involvement in the *E. coli* proteoacetylome, providing a deeper insight into this event. In the present study, we performed mass spectrometry-based profiling of proteome and lysine acetylome dynamics in *E. coli* grown under different conditions: different carbon sources, glucose (PTS carbon source) and glycerol (non-PTS carbon source); different culture media, M9 minimal medium (defined medium with inorganic ammonium-based nitrogen source) and TB7 complex medium (rich medium with peptide-based nitrogen source); and different growth stages, exponential, and stationary phases. Thus, the acetylation levels were studied in four culture media (TB7-glucose, TB7-glycerol, MM9-glucose, and MM9-glycerol), and within each condition, in two different growth phases: stationary and exponential. Quantitative label-free mass spectrometric analysis of the proteome and acetylome was performed using an Orbitrap Exploris 480 mass spectrometer. A positive correlation between protein abundance and the number and location of acetylation sites was observed under each condition, depending on the type of culture medium. Moreover, these results revealed a direct correlation between acetylation level and acetate overflow triggered by a high culture growth rate. However, a higher number of unique acetylation sites were observed in minimal media than in complex media. The enzymatic acetylation level remained residual under our conditions, likely because of the abundant chemical acetylation background. Our findings expand the knowledge on the number of acetylation sites, opening new avenues for investigation of their function. Therefore, these results represent a step forward in understanding the regulation of central metabolism by acetylation in bacteria and identifying the relative influence of the three growth conditions.

RESULTS

Relative effect of three growth factors on *E. coli* proteome analysis

Analysis of *E. coli* proteome by label-free mass spectrometry was performed to compare the relative abundance of proteins as a function of the relationships between three variables: carbon source (glucose and glycerol), type of culture medium (minimal medium, MM9, and complex medium, TB7), and growth phase (exponential and stationary phases). We obtained 8 types of samples in which the three variables or conditions were combined: MM9-glucose-exponential (MUX), MM9-glucose-stationary (MUS), MM9-glycerol-exponential (MYX), MM9-glycerol-stationary (MYS), TB7-glucose-exponential (TUX), TB7-glucose-stationary (TUS), TB7-glycerol-exponential (TYX), and TB7-glycerol-stationary (TYS) (Table S1). Samples were compared in pairs, keeping two conditions fixed while the third variable was changed, resulting in 12 comparisons: four for growth phase, MUS vs. MUX, MYS vs. MYX, TUS vs. TUX, and TYS vs. TYX; four for carbon source, MUX vs. MYX, MUS vs. MYS, TUX vs. TYX, and TUS vs. TYS; and four for culture medium, MUX vs. TUX, MUS vs. TUS, MYX vs. TYX, and MYS vs. TYS. The percentages of common and uncommon proteins among samples in which only one variable was changed were studied using Venn diagrams. The results showed that 82–92% of proteins were shared among different conditions (Figure S1). The highest number of differentially expressed proteins was observed when comparing different types of culture media. Therefore, 26 unique proteins involved in thiamine biosynthesis, enterobactin biosynthesis, and iron ion homeostasis were identified in TB7. Twenty-two unique minimal media proteins were involved in amino acid transport in addition to the glycerate 2-kinase encoded by *glxK* (Table S1).

Principal component analysis (PCA) was then conducted to check for effects and sample differences due to the variables of interest (Figure 1A). This technique simplifies the interpretation of complex data by reducing the number of variables to new ones, called components, which are ordered by the original variance of the data. The first two principal components explained 56.3% of the variance in the proteome data. Samples were grouped (right and left) based on the type of culture medium (component 1), whereas the growth phase (component 2) clustered the data up and down, and no clear grouping was observed owing to the carbon source.

Student's t-tests were performed for the same 12 comparisons as the Venn diagrams to quantify the differences in protein abundance between culture conditions. For this analysis, only the proteins present in at least three of the four biological replicates in both samples were considered. Proteome data distributions with Fch values (significant and non-significant) for 12 comparisons are shown in a boxplot (Figure 1B). Boxplots provide an overview of condition-dependent changes in protein abundance. Analysis of the proteomic data revealed that the changes in protein abundance generally became more pronounced compared to the type of culture medium in the stationary phase, with the largest interquartile distance at the extremes. In contrast, less prominent changes in protein abundance defined by the carbon source were observed (Figure 1B).
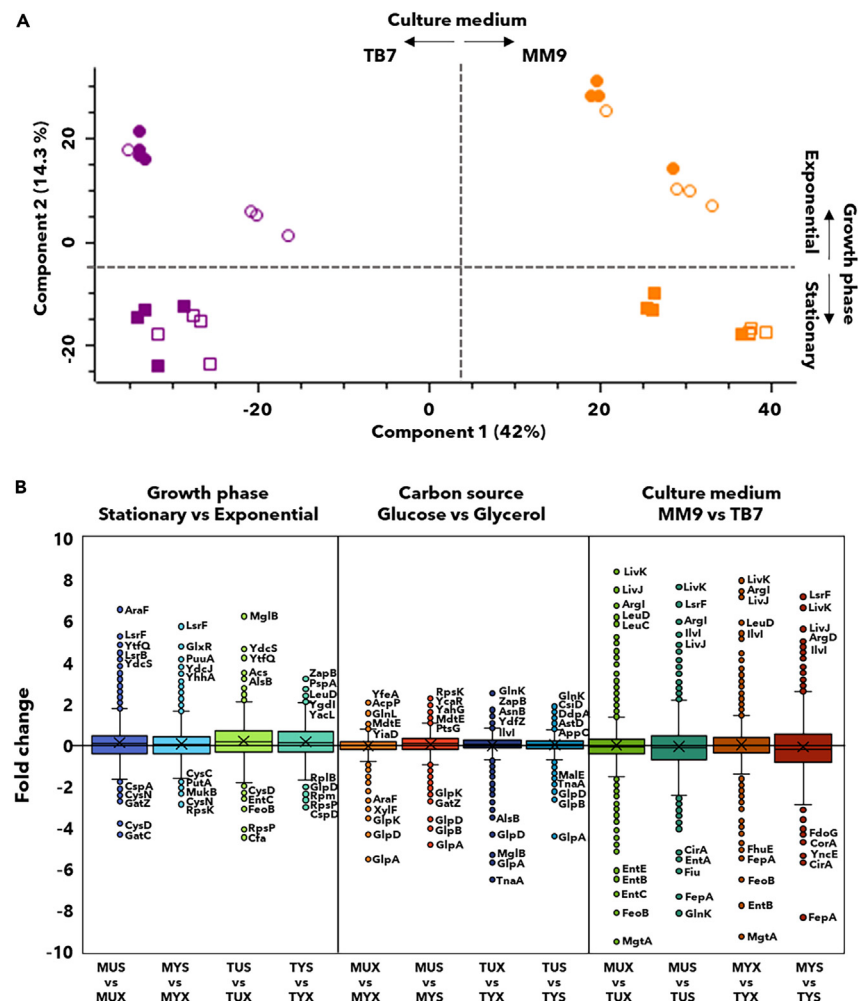
Figure 1. PCA analysis and boxplot of proteome comparisons Fch values

(A) Variables: type of culture medium (TB7 and MM9 shown in purple and orange, respectively), carbon source (glucose and glycerol shown in filled and empty symbols, respectively), and growth phase (exponential and stationary shown in circles and squares, respectively). The name of the 5 outlier proteins that change the most has been included.

(B) Fch values for the 12 comparisons grouped by the changed variable (growth phase, carbon source, and culture medium) are shown. Line inside the box represents the median of data, while X represents the mean, and bottom and top of each box represent the first and third quartiles.

For a more detailed analysis, proteins with significant differences in relative abundance and Fch values are listed in Table S2. Proteins with significant differences between conditions were those that passed the statistical correction (s0 = 0.1; FDR based on permutations ≤0.05). Total number of proteins that presented Fch ≥ +1 or ≤ −1 in each of the 12 comparisons performed are shown in Table 1. The largest changes in protein abundance were found when comparing different culture media, with a higher abundance in MM9 when comparing exponential phase samples and in TB7 when comparing stationary phase samples. Regarding the growth phase, higher protein abundance was observed in the stationary phase than in the exponential phase. This behavior was more pronounced in samples grown in the complex medium. The effect of the carbon source was less noticeable; proteins with significant differences in abundance were found only in the following corresponding comparisons: minimal medium in the stationary phase and complex medium in the exponential phase. In both cases, a higher protein abundance was observed in glycerol than in glucose (Table 1).

To identify the pathways or BPs in which proteins with different abundances between culture conditions were involved, functional enrichment of Gene Ontology (GO) terms of BPs was performed. For this analysis, data from the 12 comparisons were grouped into three groups according to different variables: carbon source, culture medium, and growth phase. Proteins found in a single condition but not in other conditions were also considered (Table S1). The most frequent GO terms that satisfied the Benjamini-Hochberg correction and the percentage of proteins with significant differences in abundance belonging to each term (enrichment) are shown in Figure 2.

Regarding the effect of the growth phase stage, proteins more abundant in the exponential phase were involved in translational functions, metabolic processes, amino acid biosynthesis, and ribosome assembly, whereas proteins that were more abundant in the stationary phase were

Table 1. Total number of proteins with significant changes in abundance between conditions

Culture medium	MUX vs. TUX	MUS vs. TUS	MYX vs. TYX	MYS vs. TYS
Fch $\geq$ +1	150	176	30	228
Fch $\leq$ −1	137	239	18	304
Growth phase	MUS vs. MUX	MYS vs. MYX	TUS vs. TUX	TYS vs. TYX
Fch $\geq$ +1	140	132	213	184
Fch $\leq$ −1	77	122	82	75
Carbon source	MUX vs. MYX	MUS vs. MYS	TUX vs. TYX	TUS vs. TYS
Fch $\geq$ +1	0	30	10	0
Fch $\leq$ −1	0	43	43	0

(Fold change (Fch) $\geq$ +1: increase in abundance; Fch $\leq$ −1: decrease in abundance). MM9-glucose-exponential (MUX), MM9-glucose-stationary (MUS), MM9-glycerol-exponential (MYX), MM9-glycerol-stationary (MYS), TB7-glucose-exponential (TUX), TB7-glucose-stationary (TUS), TB7-glycerol-exponential (TYX), and TB7-glycerol-stationary (TYS).

related to the response to oxidative stress. With regard to the carbon source, the use of glycerol led to an increase in the presence of proteins related to its transport and metabolism, the tricarboxylic acid (TCA) cycle, and the metabolism of other carbohydrate-derived compounds. The most significant medium-dependent changes in protein abundance occurred in a set of proteins involved in amino acid metabolism. Enrichment in heat response processes (mainly chaperones involved in protein catabolic processes) and thiamine biosynthesis was observed in proteins that were more abundant in TB7. Proteins that were more abundant in MM9 were involved in amino acid biosynthesis (Figure 2).

Relative effect of three growth factors on *E. coli* acetylome analysis

To determine the impact of different culture conditions on the dynamics of acetylation in *E. coli*, samples were enriched for acetylated peptides using an immunoaffinity assay prior to mass spectrometry. Lysines found to be acetylated in each sample (at least in three replicates), all acetylation sites seen, and those found to be acetylated in only one condition (glucose, glycerol, stationary phase, exponential phase, MM9, and TB7) are listed in Table S3. The number of acetylation sites, the number of proteins to which they belong, and the percentage of acetylated proteins with respect to the total proteins expressed in *E. coli* (UniProt database of *E. coli* K12 reference proteome, 4448 sequences) are shown in Table 2. The number of acetylated lysines unique to each condition (stationary phase, exponential phase, glucose, glycerol, MM9, and TB7) and the proteins to which they belong are shown in Table 2.

A total of 7482 acetylation sites belonging to 1817 modified proteins were identified. Regarding the different acetylation sites found in a single condition, the data were similar for carbon source and growth phase variables, whereas for the type of culture medium variable, a higher number of unique acetylation sites was observed in MM9 (257) than in TB7 (76) (Table 2), as well as the number of acetylated proteins. A large percentage of proteins present in each sample was detected acetylated in at least one position of one protein molecule ranging 22–30% with respect to total proteins of *E. coli* (Table 2). Furthermore, we found a high number of common acetylation sites (1638) in eight types of experimental samples (Table 2). These acetylation sites belonged to 689 proteins, which were among the most abundant in all samples (Figure S2). To determine the acetylation consensus motif, an analysis of the sequence flanking the acetylated lysine was performed using pLogo software (Figure S3A). The results indicated that negatively charged residues (D and E) were overrepresented in the regions surrounding the acetylation sites at position −1, which is in agreement with previous studies on *E. coli* and other microorganisms.[10,17,21,32,34,35] In addition, we used GO term enrichment to determine the BPs associated with the total acetylated proteins and to understand the possible consequences of acetylation (Figure S3B). Acetylated proteins are involved in a wide range of BPs, most of which involve translation and amino acid biosynthesis. This result is similar to that found for different lysine acetylomes of diverse microorganisms.[33,35–38]

PCA of all samples allowed clear grouping of the data according to the type of culture medium and growth phase (Figure 3). The first three principal components were able to explain 49.3% of the variance in analyzed data; component 2 enabled a clear clustering of data according to culture medium, whereas component 3 enabled grouping according to growth stage (Figures 3A–3C). However, the samples were not grouped based on carbon source. Because the variable with the most differentiated samples was the culture medium, PCA analyses were also performed separately on MM9 and TB7 samples (Figures 3D and 3E). Component 2 visibly distinguished data by growth phase in both cases, but only in MM9 did sample component 1 cluster data by carbon source. To further explore the differences between samples, Venn diagrams, including the total acetylated peptides of each sample, were constructed (Figures 3F–3H). As in PCA analysis, the largest variations were found in the identity of acetylated lysines between minimal medium and complex medium, where only approximately 51–60% of acetylation sites were shared.

Relative effect of three growth factors on acetylation level for common sites

To better understand the variations in acetylation levels between different culture conditions, we decided to relatively quantified the acetylation changes in common lysines. For this purpose, a statistical analysis of the 12 comparisons (MUS vs. MUX, MYS vs. MYX, TUS vs. TUX, TYS vs. TYX, MUX vs. MYX, MUS vs. MYS, TUX vs. TYX, TUS vs. TYS, MUX vs. TUX, MUS vs. TUS, MYX vs. TYX, and MYS vs. TYS) was performed using
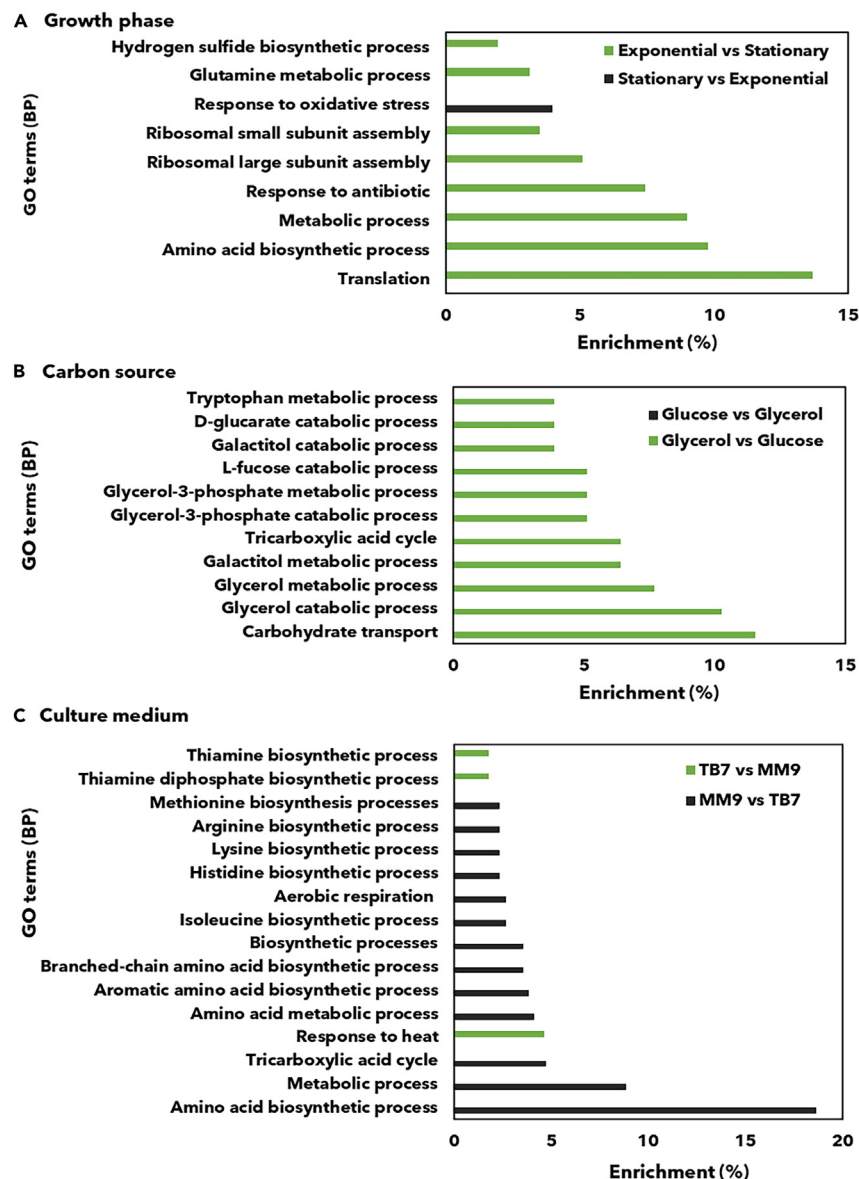
Figure 2. Enrichment in GO terms (biological processes, BP) of proteins significantly more abundant in the different study conditions
(A) GO terms with higher percentage among significantly more abundant proteins in stationary phase than in exponential phase, and vice versa.
(B) GO terms with higher percentage among significantly more abundant proteins in glucose than in glycerol, and vice versa.
(C) GO terms with higher percentage among significantly more abundant proteins in MM9 than in TB7, and vice versa.

the Student's t-test. The scatterplots of the relative intensity (log2 transformed) of the 12 comparisons are shown in Figure S4. Acetylated lysines present in at least three of the four biological replicates were considered. The acetylome data distributions with Fch values (significant and non-significant) for the 12 comparisons are illustrated in boxplots (Figure 4). Comparisons between culture media, MM9, and TB7, showed the most significant differences in the relative acetylation level, especially when growing on glucose in the stationary phase and on glycerol in the exponential phase. However, the influence of the carbon source on the acetylation level was more noticeable in minimal media than in complex media.

Then, data were filtered by selecting acetylated lysines with significant differences between conditions that passed the statistical correction (s0 = 0.1; FDR based on permutations ≤0.05) and presented a Fch ≥ + 1 or ≤ −1. The data are presented in Table S4. The number of acetylated lysines with significant differences found in each of the 12 comparisons and the proteins to which they belonged are shown in Table 3.

The number of common sites with increased acetylation levels was higher in TB7 than in MM9 in all comparisons except for the exponential phase with glucose (Table 3). Regarding the growth phase comparisons, a higher relative acetylation level in the stationary phase was

Table 2. Acetylation sites and acetylated proteins found in total, in common, and in each type of sample, and % of acetylated proteins with respect to total proteins expressed in *E. coli*

	Acetylation sites	Acetylated proteins	% Acetylated proteins
Total	7482	1817	40.84%
Common	1638	689	15.49%
MM9 glucose exponential	4342	1277	28.71%
MM9 glucose stationary	4662	1334	29.99%
MM9 glycerol exponential	4207	1276	28.69%
MM9 glycerol stationary	3406	1097	24.66%
TB7 glucose exponential	3487	1130	25.40%
TB7 glucose stationary	3581	1212	27.25%
TB7 glycerol exponential	2872	1016	22.84%
TB7 glycerol stationary	3694	1267	28.48%

	Growth phase		Carbon source		Culture medium	
	Stationary	Exponential	Glucose	Glycerol	MM9	TB7
AcK	13	16	9	9	257	76
Proteins	13	16	8	8	171	59

Number of unique acetylation sites (AcK) found in a single culture condition and proteins (Proteins) they belong to.

observed in the TB7-glucose samples, and the opposite behavior was exhibited by the MM9-glycerol samples. However, the level of acetylation was the same in both growth phases in the MM9-glucose and TB7-glycerol media, as no changes were observed. With regard to carbon source, no significant differences in acetylation levels were observed in the TB7 samples. Nevertheless, in the MM9 samples, glucose supplementation led to an increase in acetylation, which was higher in the stationary phase. Accordingly, the increase in the acetylation levels derived from glucose utilization also depended on the culture medium. In summary, the data obtained suggest that acetylation levels strongly depend on the type of culture medium used. However, acetylation was also affected by the supplemented carbon source only in minimal medium. These results are consistent with those of our previous exploratory analyses (Figures 3D and 3E).

To identify biological pathways or processes involving proteins with significant changes in acetylation levels under different conditions (grouped by variables: growth phase, carbon source, and type of culture medium), GO term enrichment of BPs was performed. The 15 most abundant GO terms that satisfied the Benjamini-Hochberg correction are shown in Figure 5. By comparing the processes in which proteins with different acetylation levels between growth phases were involved, we observed that proteins exhibiting a higher acetylation level in the exponential phase were related to translation and central carbon metabolism processes, such as the TCA cycle, glycolytic processes, and glyoxylate cycle. Regarding variations in the functions of differentially acetylated proteins grown on the two carbon sources, the presence of glucose triggered an increase in the acetylation levels of proteins involved in translation processes, amino acid biosynthesis, ribosome assembly, tRNA aminoacylation for translation, and certain processes of central carbon metabolism. A high percentage of proteins with an increase in the number of acetylated sites in MM9 were related to general amino acid, aromatic, and branched-chain amino acid biosynthesis, whereas proteins with an increase in the level of acetylated lysine in TB7 than in MM9 were enriched in gluconeogenesis, purine nucleotide biosynthesis, and heat response (Figure 5).

Analysis of extracellular acetate concentration and specific growth rate of *E. coli* under different growth factors

Accumulating evidence from *E. coli* acetylome studies has linked non-enzymatic acetylation to acetate metabolism through an acetyl-P-dependent mechanism.[10,19] To determine whether changes in acetylation level comparing growth factors were related to acetate overflow, extracellular concentration of this metabolite was measured, and maximum specific growth rate (μ_{max}) was calculated. For this purpose, *E. coli* K12 strain was grown in MM9 or TB7 supplemented with glucose or glycerol as the carbon source, and cell growth was monitored by OD measurements. The cell growth and extracellular concentrations of acetate, glucose, and glycerol are shown in Figure S5. The specific growth rate data are shown in Table 4, and the maximum values of extracellular acetate under each condition are shown in Figure 6.

The specific growth rate was higher in the complex medium than in the minimal medium, and in glucose than in glycerol, which was more influenced by the type of medium than by the carbon source. Simultaneously, glucose consumption was lower in complex medium while glycerol consumption was similar in both growth media (Table 4). In all types of cultures, acetate was excreted during the exponential phase, but its reincorporation after depletion of the carbon source occurred at different growth times. Specifically, in the TB7-glucose cultures, acetate was reincorporated at the beginning of the stationary phase. In the TB7-glycerol and MM9-glucose cultures, acetate reincorporation occurred during the late exponential phase (Figure S5). The maximum extracellular acetate concentration was observed in the samples grown in TB7-glucose (15.89 mM), followed by those grown in TB7-glycerol (11.91 mM). However, growth in glucose-containing minimal medium resulted in
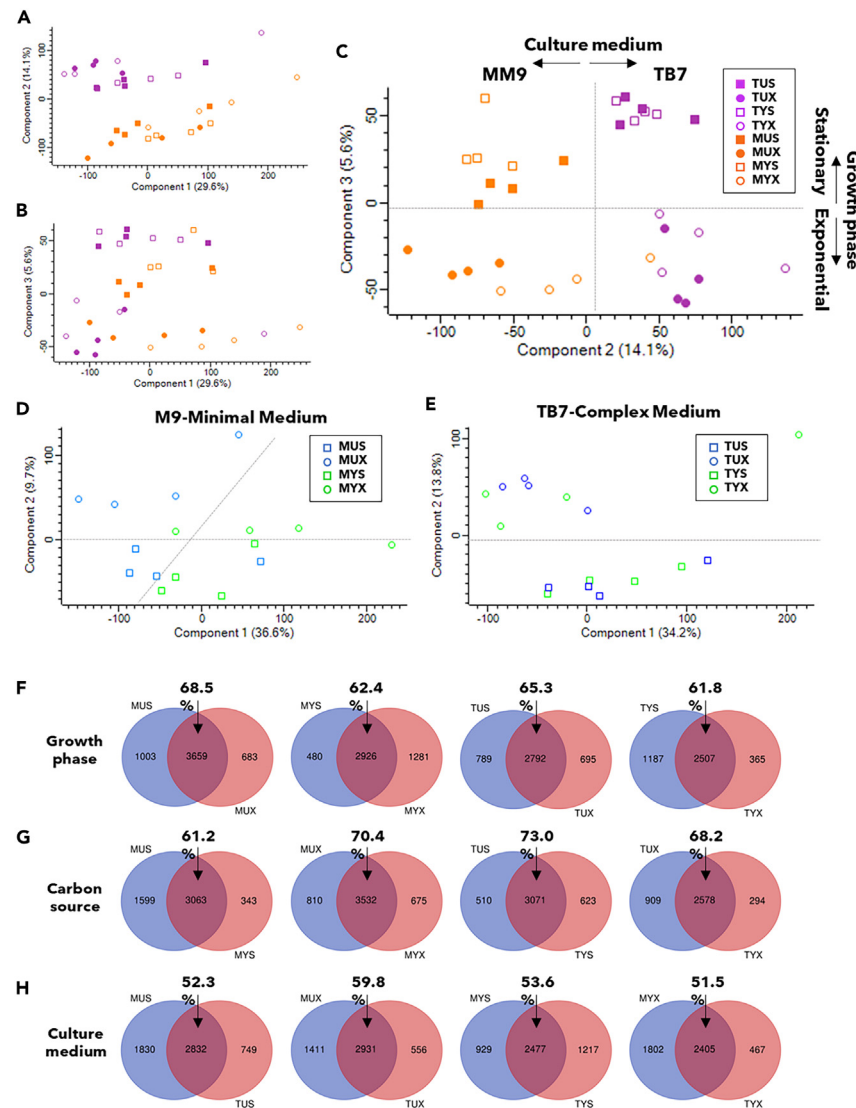
Figure 3. PCA analysis and Venn diagrams of normalized acetylome data

(A–C) Variables: type of culture medium (TB7 and MM9 shown in purple and orange, respectively), carbon source (glucose and glycerol shown in filled and empty symbols, respectively), and growth phase (exponential and stationary shown in circles and squares, respectively). (A) Component 1 vs. Component 2. (B) Component 1 vs. Component 3. (C) Component 2 vs. Component 3.

(D and E) Samples were classified by culture medium, MM9 (D) and TB7 (E). Carbon source, glucose and glycerol, are shown in blue and green, respectively, and growth phase, exponential and stationary, are shown in circles and squares, respectively.

(F–H) Comparisons of acetylated lysines of samples varying growth phase (F), carbon source (G), and type of culture medium (H). Percentages corresponding to number of acetylated lysines identical between two conditions compared.

a 2.6-fold reduction in acetate concentration compared to TB7-glucose samples and in the MM9-glycerol culture acetate excretion was almost negligible (0.93 mM) (Figure 6). In addition, the extracellular acetate concentration in minimal medium was more dependent on the carbon source than on TB7. Consequently, the higher acetate concentration in TB7 was consistent with previous results related to an increased acetylation level (Table 3, refer to culture medium), whereas in minimal medium, the acetylation level was higher when glucose was used as the carbon source (Table 3, see carbon source). Collectively and with previous results (Figure 4; Table 3), these data reaffirm the link between acetate metabolism and extensive acetylation level.[10,17,19]

Study of acetylation sites regulated by enzymatic acetylation

A previous study by Christensen et al.[39] demonstrated that in *E. coli*, there are other acetyltransferases besides PatZ (also called Pka and YfiQ), such as YiaC, YjaB, RimI, and PhnO, which show specificity for their acetylated sites. To discriminate enzymatic acetylation from global
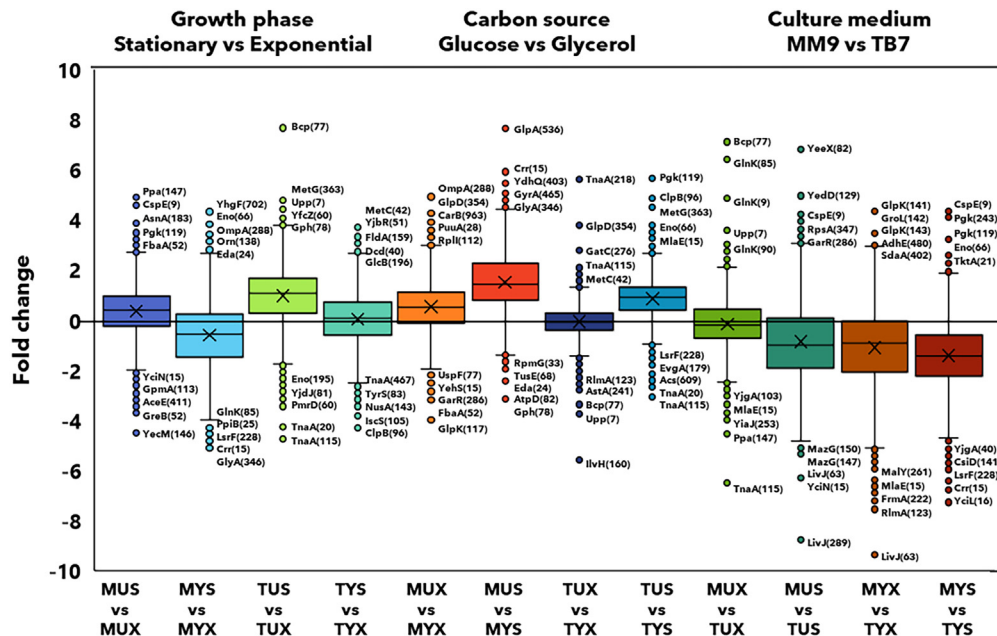
Figure 4. Boxplots of acetylome comparisons Fch values (significant and no significant) for the three variables, growth phase, carbon source and culture medium

Line inside the box represents the median of data while X represents the mean, and bottom and top represent the first and third quartiles. The name of the 5 outlier proteins that change the most has been included.

acetylation, we compared the acetylation sites regulated by acetyltransferases found by Christensen et al.[39] with the acetylation sites identified in our study in each of the eight experimental samples (Table S3). In total, 128 lysines (5.9–7.3% of acetylation sites in our study) were regulated by acetyltransferases (Table S5). This low level of enzymatic acetylation has been described previously.[10,16] The acetylation levels of these lysines were compared under different growth conditions, and those with significant changes are shown in Table 5. These acetylation sites have been reported to belong to proteins associated with translation and the regulation of translation processes (Figure 7). Regarding the percentages that these lysines represented with respect to the total differentially acetylated lysines in each condition, we observed higher values of enzymatically acetylated lysines in the exponential phase than in the stationary phase in growth phase comparisons. We also noticed a larger percentage of acetyltransferase-regulated acetylation sites (18.58% and 17.65%) with an increase in the level of acetylation in MM9 than in TB7 (Table 5). When comparing the identity of the peptides acetylated by acetyltransferases with the specificity results established by Christensen et al.,[39] PatZ-regulated sites were shown to be the most prevalent, followed by YiaC and YjaB. We only detected two sites regulated by PhnO and none by RimI (Table 5), demonstrating a minimum redundancy among the targets, as previously found.[39] This dataset provides valuable information for evaluating the impact of enzymatic acetylation on a large background of nonenzymatic acetylation.

Analysis of acetylation on central metabolism of *E. coli* under different culture conditions

Functional analysis by GO enrichment revealed the prevalence of differentially acetylated proteins related to translational processes and central metabolism of the bacterium (Figure 5), as reported in other studies.[17,19,40,41] Thus, we focused on enzymes with differentially acetylated lysines involved in central carbon metabolism (glycolysis, gluconeogenesis, TCA cycle, glyoxylate cycle, acetate metabolism, anaplerotic reactions, pentose phosphate pathway, and PTS system) and ammonium assimilation pathways (Table S6; Figure S6).

Most of the proteins belonging to these central metabolic pathways were acetylated under at least one culture condition (Table S3), and 59 enzymes were reported to show significant changes in acetylation levels between conditions (Figure S6). Proteins with lysines showing an increase in the level of acetylation in the stationary phase compared to that in the exponential phase were overrepresented in glycolysis and the pentose phosphate pathway, with the enzymes phosphoglycerate kinase (Pgk) and transketolase (TktA and TktB) presenting ten lysines with higher acetylation levels. In contrast, enzymes with lysines showing an increase in the level of acetylation in the exponential phase were mainly involved in the TCA and glyoxylate cycles (Figure S6A). Only three lysines corresponding to glycerol-3-phosphate dehydrogenase (GlpD), glyceraldehyde-3-phosphate dehydrogenase (GapA), and phosphoenolpyruvate carboxykinase (PckA) were found to have higher acetylation levels in glycerol; therefore, these acetylation sites could be specific to glycerol use. Enzymes with acetylated lysines triggered by glucose were distributed throughout the central metabolic pathways, although to a greater extent in the PTS system (six acetylation sites in enzyme I, EI), TCA cycle (six acetylation sites in isocitrate dehydrogenase, Icd), and glycolysis (six acetylation sites in pyruvate kinase, PykAF) (Figure S6B).

Table 3. Number of common acetylated lysines (AcK) with significant changes in relative acetylation level between conditions and proteins to which they belong

Culture medium	MUX vs. TUX	MUS vs. TUS	MYX vs. TYX	MYS vs. TYS
AcK (Fch ≥ +1)	0	183	34	1
Proteins (Fch ≥ +1)	0	139	31	1
AcK (Fch ≤ −1)	0	881	533	69
Proteins (Fch ≤ −1)	0	481	343	65
Growth phase	**MUS vs. MUX**	**MYS vs. MYX**	**TUS vs. TUX**	**TYS vs. TYX**
AcK (Fch ≥ +1)	0	22	396	0
Proteins (Fch ≥ +1)	0	22	264	0
AcK (Fch ≤ −1)	0	177	19	0
Proteins (Fch ≤ +1)	0	133	19	0
Carbon source	**MUX vs. MYX**	**MUS vs. MYS**	**TUX vs. TYX**	**TUS vs. TYS**
AcK (Fch ≥ +1)	30	676	0	0
Proteins (Fch ≥ +1)	28	367	0	0
AcK (Fch ≤ −1)	0	1	0	0
Proteins (Fch ≤ −1)	0	1	0	0

(Fold change (Fch) ≥ +1: increase in abundance; Fch ≤ −1: decrease in abundance). MM9-glucose-exponential (MUX), MM9-glucose-stationary (MUS), MM9-glycerol-exponential (MYX), MM9-glycerol-stationary (MYS), TB7-glucose-exponential (TUX), TB7-glucose-stationary (TUS), TB7-glycerol-exponential (TYX), and TB7-glycerol-stationary (TYS).

Regarding the comparison between culture media types, we observed the highest number of differentially acetylated lysines among all variables analyzed (Figure S6C). Lysine residues with increased acetylation in TB7 belong to the glycolysis and pentose phosphate pathways. Specifically, PykAF, pyruvate dehydrogenase complex (Pdh), and TktAB enzymes showed 9, 19, and 10 lysines, respectively, with a higher level of acetylation in TB7 (Figure S6C). Differentially acetylated lysines in MM9 were less abundant and were mainly concentrated in the TCA cycle, some enzymes involved in nitrogen metabolism, the glyoxylate cycle, anaplerotic reactions, and enzymes of the final part of glycolysis.

To determine whether the differences in acetylation levels between the different conditions identified by MS/MS showed biological functionality, we chose three enzymes (GapA, glyceraldehyde dehydrogenase; Mdh, malate dehydrogenase; AceA, isocitrate lyase) and measured their activity in the cell extracts (Figure 8). These enzymes were chosen because their activity is known to be regulated by acetylation[21,40,42,43] and regulatory lysines were found to be differentially acetylated in this study (Table S4). *E. coli* K12 strain was grown in the culture media where these differences were observed (Figure S5). One-way ANOVA was performed to identify significant differences between relative enzymatic activities. The identity and localization of studied lysines is showed in their three-dimensional structure (Figure 8).

GapA showed 23.84% higher activity in TB7-glucose in stationary phase than under the same conditions in minimal medium. The enzyme from the TCA cycle, Mdh, was a 54.32% less active in MYX than in TYX. Acea, a glyoxylate cycle enzyme, was a 49.46% more active in MM9-glucose during stationary phase than in TB7-glucose during the same growth phase (Figure 8).

DISCUSSION

Nε-lysine acetylation is related to metabolic and energetic state of the bacterium through acetyl-CoA and acetyl-P intermediates; therefore, nutritional and culture conditions are determining factors in the abundance of this PTM.[4,10,16] The present study reveals the relative impact of three different culture conditions on proteoacetylome in *E. coli*, using label-free quantitative mass spectrometry. Thus, we used a PTS carbon source, glucose, which is preferentially used by bacteria because of its higher metabolic value,[44,45] and a non-PTS carbon source, glycerol, which is important for biotechnological resource utilization.[22,46] Two culture media were alternatively employed: a defined medium based on inorganic ammonium, MM9, and a rich medium based on peptides, amino acids, and nucleotides, TB7. Finally, the influence of growth stage on protein abundance and acetylation was studied by analyzing samples taken at the exponential and stationary *E. coli* growth phases. The relationship of this PTM with the carbon source and growth phase in an independent manner has been previously studied in *E. coli* and other microorganisms.[10,16,17,19,30,47] However, when a culture is performed, several factors simultaneously influence metabolism and its regulation; therefore, a study of the dynamics of acetylation that encompasses different cultural factors is needed.

Approximately 82–92% of the observed proteins were shared between samples (Figure S1), and few exclusive proteins were associated with only one variable were detected (Table S1). Focusing on the differences in the proteome between growth conditions, PCA analysis and boxplots (Figure 1) showed a clear clustering of the samples by the effect of culture medium, followed by growth phase, while the carbon source showed limited influence. GO analysis of the proteome comparison between the minimal medium and nutrient-rich medium showed the largest changes in proteins related to amino acid biosynthesis (Figures 2 and S7). The presence of amino acids entering the central carbon metabolism from different positions may have a cumulative effect, leading to increased acetate excretion, while their absence would indicate
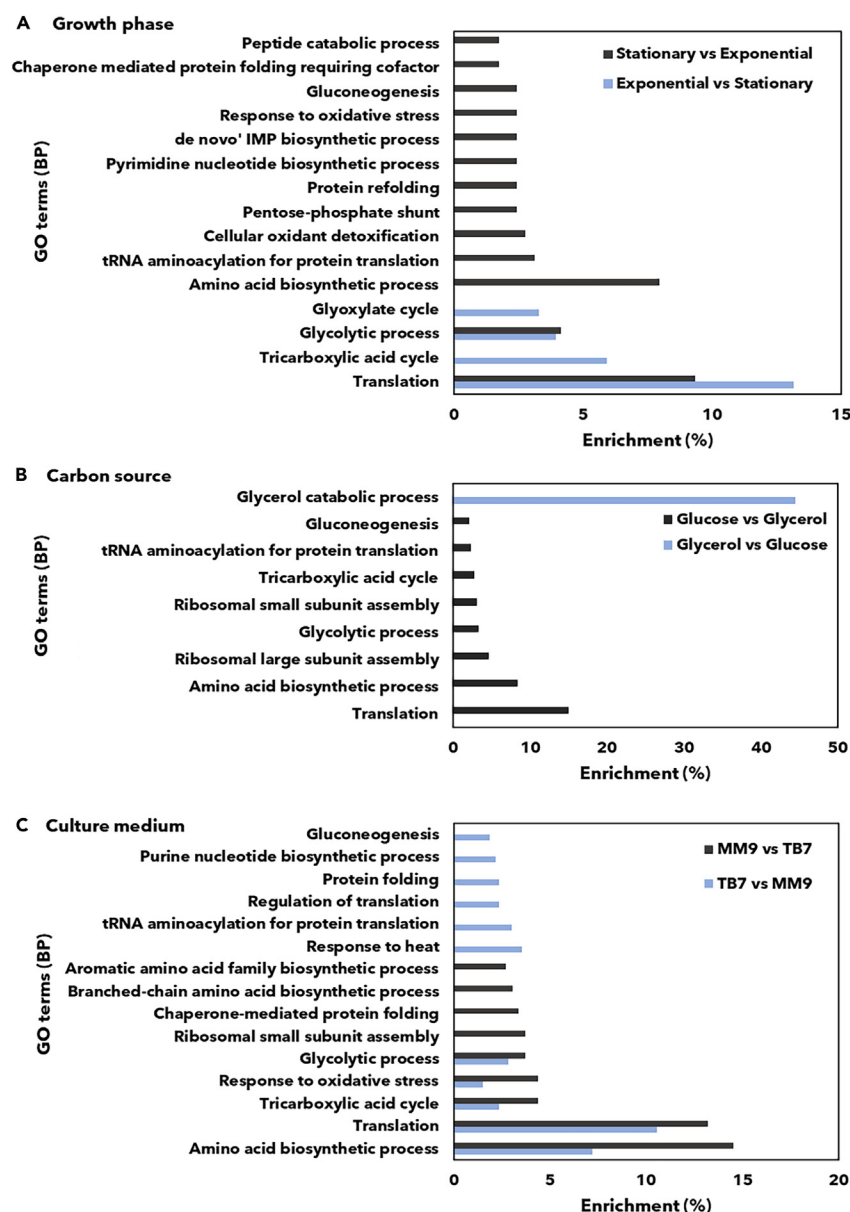
Figure 5. Enrichment in GO terms (biological processes, BP) of proteins with significantly more abundant acetylation sites in the different study conditions

(A) GO terms with higher percentage of proteins with lysines with a significant increase of acetylation in stationary phase than in exponential phase, and vice versa.

(B) GO terms with higher percentage of proteins with lysines with a significant increase of acetylation in glucose than in glycerol, and vice versa.

(C) GO terms with higher percentage of proteins with lysines with a significant increase of acetylation in MM9 than in TB7, and vice versa.

a redistribution of precursors toward biosynthetic processes.[48] Our data agree with a proteome redistribution that promotes acetate formation through the Pta-AckA pathway under nutrient-rich conditions (Figures 6 and S7; Table S2), whereas the acetate-consuming enzyme Acs (acetyl-CoA synthetase) and proteins of the TCA and glyoxylate cycles were more abundant in the minimal medium (Figure S7; Table S2). This redistribution results in a higher excretion of acetate in complex media, as shown (Figures 6 and S5), and a higher flux through the TCA cycle to obtain intermediates for biosynthetic pathways in minimal media.

In the growth phase, proteins with significant changes were more abundant in the stationary phase than in the exponential phase in all comparisons, and this pattern was more noticeable in the TB7 samples (Figure 1B; Table 1). The higher abundance of proteins in TB7 in the stationary phase can be explained by the transition to the growth phase, which involves a dynamic reorganization of the central metabolism in response to substrate starvation.[23] The regulatory responses to different carbon sources were moderate, although we found a

Table 4. Specific growth rates (μ_{max}) and specific carbon consumption rates (q_s) for *E. coli* K12 strain growing in different culture conditions

	TB7-glucose	TB7-glycerol	MM9-glucose	MM9-glycerol
μ_{max} (h^{-1})	1.15 ± 0.08	0.92 ± 0.06	0.71 ± 0.04	0.59 ± 0.02
q_s (mmol gDCW^{-1})	9.51 ± 0.38	16.49 ± 0.63	12.34 ± 0.50	15.77 ± 0.63

higher abundance of common proteins in response to carbon catabolic repression[49,50] (Table 1; Figure 1B). This was confirmed by functional analysis of GO terms, as we observed an enrichment of proteins related to glycerol and other carbohydrate metabolism, carbohydrate transport, and the TCA cycle among the proteins more abundant in glycerol (Figure 2), which is supported by other authors.[51,52]

Total number of acetylated lysines found under all conditions was 7482, belonging to 1817 proteins, indicating that 51–71% of the proteins detected in our study were acetylated in at least one position; therefore, approximately 22–30% of total *E. coli* proteins may be acetylated in at least one lysine (Table 2). The number of acetylation sites found in this study was high despite not using conditions that trigger an increase in acetylation levels (CobB sirtuin-deficient strains, overexpression of any lysine acetyltransferase, or *ackA* gene-deficient strains).[10,16,21,30,39,53] This could be due to the simultaneous use of three different variables (carbon source, growth phase, and culture medium), which increases the number of differences in protein abundance (Table 1; Figure 1), combined with a high-throughput screening technology such as the Exploris 480 mass spectrometer. First, PCA of the normalized acetylome data showed clustering by media type and growth phase (Figure 3). These results were similar to those of the proteome analysis, but with less pronounced variable dependencies. Moreover, dependence on the sugar source was observed only in the minimal medium samples. (Figure 3E). Next, we observed that the fraction of acetylated proteins was correlated with protein abundance (Figure S2). In this sense, several common acetylation sites were detected in all samples, representing approximately 35–57% of the total number of acetylation sites, being the percentage higher in complex media (Table 2). With respect to differences in the localization of the modified lysines, the results showed that, the number of unique acetylation sites detected was higher in a defined medium than in a complex medium (Table 2). In view of these results, the differential localization of acetylation sites between media can be explained, in part, by the relative abundance of proteins. However, there must be more factors that account for the higher number of individual acetylation sites found in MM9, which seem to respond to specific acetylation in this medium.

To explore the acetylation-dependent mechanisms in more detail, the differences in the relative lysine acetylation levels between culture conditions were analyzed using Student's t-test on acetylome samples. It is well known that non-enzymatic acetylation is driven to a large extent by concentration of acetyl-P, which in turn, depends on acetate overflow metabolism.[8] Based on the foregoing, we analyzed the acetylome comparisons shown in Figure 4 and Table 3, growth curves, and extracellular acetate concentrations under different culture conditions (Figures 6 and S5). Collectively, these results demonstrated a close link between acetylation levels and acetate overflow in fast-growing cultures. The relative level of acetylation with significant changes depended on the maximum extracellular concentration of acetate detected and the growth phase in which acetate uptake occurred. Therefore, the relative acetylation level was higher in the complex medium than in the minimal medium, and this relative acetylation level was observed in the stationary phase of growth on TB7-glucose when the reincorporated acetate was metabolized (Table 3; Figure S5). In contrast, no differences in the relative levels of acetylation were observed when comparing the growth phases under conditions in which the incorporation of acetate occurred during the exponential phase, indicating that most of the acetylation points were of long duration without dynamic rotation (Table 3, MUS vs. MUX and TYS vs. TYX). Integrating the proteome data, we observed that Acs abundance increased during glucose starvation in the stationary phase in TB7-glucose, and in the exponential phase in TB7-glycerol and MM9-glucose (Table S2). Another significant difference that would explain acetate overflow in the exponential phase of growth on TB7 glycerol medium was tryptophanase (TnaA, Fch = 6.54) overabundance involved in pathway II of L-tryptophan degradation (pyruvate pathway), which is subject to catabolic repression by TB7 glucose. In addition, we observed a faster consumption of glycerol than glucose in the complex medium (Table 4). In contrast, the relative acetylation levels were more dependent on the sugar source in the defined medium (Figure 6). Thus, although the acetylation level in MM9-glucose was linked to acetate production, this relationship was not observed in MM9-glycerol because these are slow-growing cell cultures with balanced metabolic pathways.

Continuing with the factors involved in lysine acetylation, we noted that the enzymatic acetylation level was residual under these experimental conditions. By comparing our data with those of Christensen et al.,[39] we observed that only 6.83% of the differentially acetylated sites
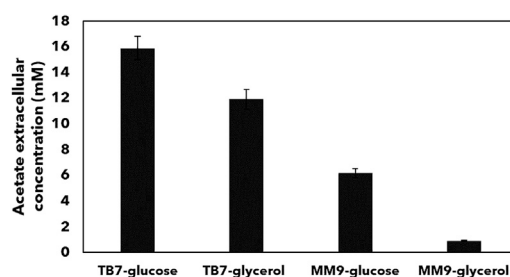
Figure 6. Maximum extracellular acetate concentration of *E. coli* K12 growing in different culture conditions
Data are presented as mean ± SD (n = 4).

Table 5. Number of acetylated lysines (AcK) with significant differences that are common to acetylation sites regulated by an acetyltransferase in Christensen et al. (2018)

Culture medium	MUX vs. TUX	MUS vs. TUS	MYX vs. TYX	MYS vs. TYS
AcK (Fch ≥ +1)	–	34	6	0
% (Fch ≥ +1)	–	18.58%	17.65%	–
AcK (Fch ≤ −1)	–	30	24	4
% (Fch ≤ −1)	–	3.41%	4.50%	5.80%
Growth phase	**MUS vs. MUX**	**MYS vs. MYX**	**TUS vs. TUX**	**TYS vs. TYX**
AcK (Fch ≥ +1)	–	2	12	–
% (Fch ≥ +1)	–	9.09%	4.05%	–
AcK (Fch ≤ −1)	–	26	5	–
% (Fch ≤ +1)	–	14.69%	26.32%	–
Carbon source	**MUX vs. MYX**	**MUS vs. MYS**	**TUX vs. TYX**	**TUS vs. TYS**
AcK (Fch ≥ +1)	3	69	–	–
% (Fch ≥ +1)	10.00%	10.19%	–	–
AcK (Fch ≤ −1)	–	0	–	–
% (Fch ≤ −1)	–	–	–	–

	PatZ	YjaB	YiaC	RimI	PhnO
Nº of AcK	96	27	58	0	2

Percentage (%) that these acetylation sites represent with respect to the total differentially acetylated sites of each condition. Acetyltransferases found by Christensen et al. (2018)[39] and number of common acetylation sites (Nº of AcK) regulated by these acetyltransferases and found in our study. (Fold change (Fch) ≥ +1: increase in abundance; Fch ≤ −1: decrease in abundance). MM9-glucose-exponential (MUX), MM9-glucose-stationary (MUS), MM9-glycerol-exponential (MYX), MM9-glycerol-stationary (MYS), TB7-glucose-exponential (TUX), TB7-glucose-stationary (TUS), TB7-glycerol-exponential (TYX), and TB7-glycerol-stationary (TYS).

were acetyltransferase-regulated sites (Table S5), and functions of the proteins to which they belonged were focused on translation (Figure 7), so this type of acetylation may have a more relevant role in this process and its regulation. Moreover, the differences in acetylation due to acetyltransferase activity were more relevant in MM9-glycerol and in the exponential phase which could explain the acetylation dynamics detected in this growth medium (Figure 4; Tables 3 and 5). Neither of the acetyltransferases were found to differ significantly in abundance, but we observed that PatZ, which plays a major role in acetylation (Table 5), was more abundant in MM9 samples than in TB7 samples (Table S1). This could explain some of the differences in the unique modified lysines in MM9, in addition to the differential abundance of the medium-related proteins mentioned above.

To determine whether differences in the level of acetylation affect the flux of central metabolism, the activities of three enzymes regulated by acetylation, GapA, Mdh, and AceA, were measured. GapA activity was inhibited by chemical acetylation at lysine 184 in *E. coli*[40] and was found to be significantly more acetylated in the MM9-glucose stationary phase than in the TB7-glucose stationary phase (Table S4), which is consistent with the lower activity observed in MUS than in TUS in the cell extract (Figure 8). Malate dehydrogenase showed increased activity when acetylated at residues K99 or K140.[42] In the present study, K140 showed a higher level of acetylation in TB7 than in MM9 (Table S4), this increase in the level of acetylation was related to a higher activity in complex media (Figure 8). AceA activity is reduced when acetylation level is increased, a previous study, that proved this loss of activity, found lysines 13, 34, 308, 326, and 331 acetylated.[21] Another study showed that acetylation of *Mycobacterium tuberculosis* lysine 322, which is homologous to K326 in *E. coli*, resulted in the reduced activity of this enzyme.[43] The activity of AceA was higher in minimal medium than in complex medium (Figure 8), and we observed a higher level of acetylation of lysines
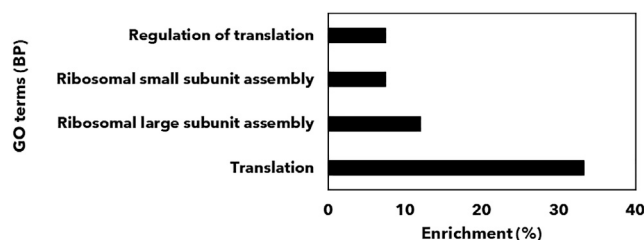

Figure 7. GO enrichment (biological processes, BP) of proteins with acetylated lysines regulated by acetyltransferases
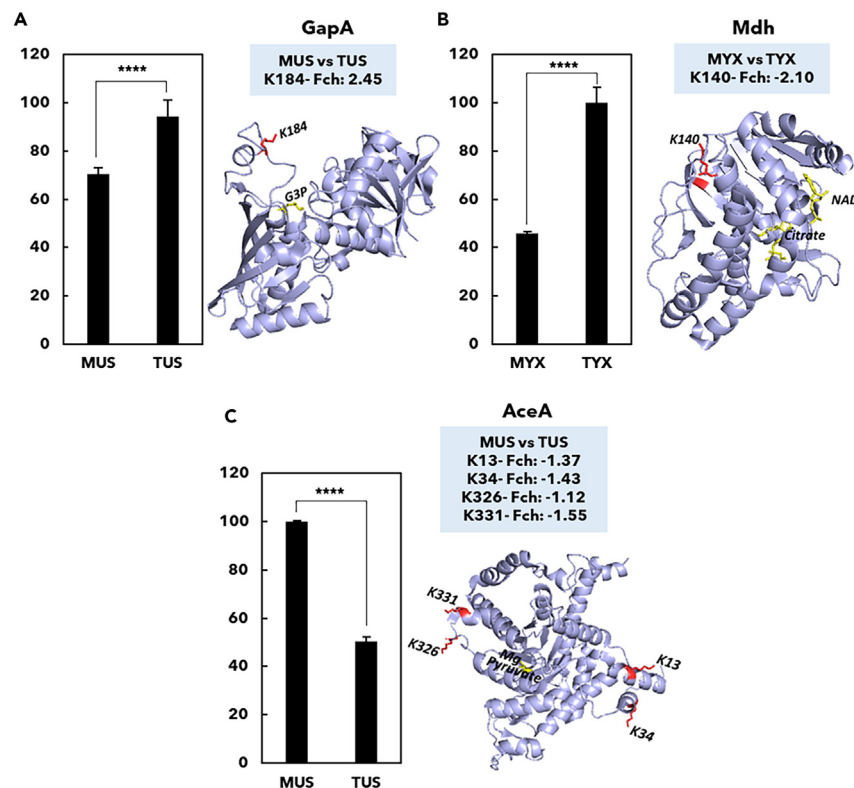
Figure 8. Relative enzymatic activity of enzymes measured in cell extracts
(A) GapA enzymatic activity.
(B) Mdh enzymatic activity.
(C) AceA enzymatic activity.
Enzyme activities relativized to the sample with the highest activity (100%). MM9-glucose-stationary (MUS), MM9-glycerol-exponential (MYX), TB7-glucose-stationary (TUS), and TB7-glycerol-exponential (TYX). Acetylate lysines with significant differences and its Fold change (Fch) appear in the blue square. Protein structures with substrate binding site and Ack sites are shown (PDB: 1dc4, 1emd, 1igw). Data are presented as mean $\pm$ SD (n = 3). A one-way ANOVA test was carried out to identify significant differences between relative enzymatic activities (p value <0.0001 (****), <0.001 (***), <0.01 (**), and <0.05(*)).

13, 34, 326, and 331 in TB7 than in MM9 (Table S4), suggesting that acetylation of these sites could be the cause of lower activity in complex media (Figure 8). Therefore, the use of different culture media may induce differential acetylation of these enzymes, which could determine the fine regulation of the fluxes of these interconnected pathways. Based on these results, we propose possible acetylation targets involved in the highlighted metabolic pathways with potential functional effects listed in Table S6, which may provide a starting point for the discovery of new regulations, the physiological relevance of which must be assessed on an individual basis.

The results of our study contribute to the advancement of knowledge on lysine acetylation in *E. coli* as a model microorganism and an important cell factory. The most relevant conclusions are as follows: (1) The type of medium (rich or defined) is the main determinant of both protein abundance and acetylation, with acetylation being higher in complex media than in defined media. However, the number of single acetylated sites was higher in minimal medium, suggesting a higher specificity, which could be due to the higher enzymatic acetylation identified in this study; (2) acetylated proteins were among the most abundant proteins in all samples; and (3) the acetylation level and acetate overflow were closely linked, with acetylation mainly irreversible if it occurred during the exponential phase because no dynamics of acetylation were observed.

The culture medium is one of the most influential parameters in biotechnological processes. Several studies have demonstrated the importance of the type of medium and carbon source for the production of highly valuable compounds[54–58] in *E. coli*. Moreover, as demonstrated in this and previous studies,[59,60] culture conditions are a determining parameter for the identity and level of protein acetylation, which is essential for the development of processes to produce recombinant proteins or other compounds of industrial interest. The results of this study provide valuable information regarding the use of culture conditions as a tool to modulate metabolism in processes using *E. coli* as a cellular factory.

Limitations of the study

This study has some limitations related to the technique used, mass spectrometry.

Peptides smaller than 6 amino acids or with a mass greater than 5600 Da are not detected, so the coverage of the proteins is not 100%, although good values are obtained. Also, for this reason, not all acetylations that may occur are detected, only those found in peptides that comply with these conditions.

Proteins with very low abundance are more complex to detect.

STAR★METHODS

Detailed methods are provided in the online version of this paper and include the following:

- KEY RESOURCES TABLE
- RESOURCE AVAILABILITY
  - Lead contact
  - Materials availability
  - Data and code availability
- EXPERIMENTAL MODEL AND STUDY PARTICIPANT DETAILS
- METHOD DETAILS
  - Cell cultures and acetylated peptide enrichment
  - LC-MS parameters
  - Data analysis
  - Cell growth and acetate concentration analysis
  - Enzymatic assay
- QUANTIFICATION AND STATISTICAL ANALYSIS

SUPPLEMENTAL INFORMATION

Supplemental information can be found online at https://doi.org/10.1016/j.isci.2024.109017.

AUTHOR CONTRIBUTIONS

Conceptualization, G.L.-T., J.G.-J., and T.D.d.P.; Methodology, G.L.-T., J.G.-J., R.A.S.-M., A.M.V., R.Z.C., and A.J.R.H.; Investigation, G.L.-T., J.G.-J, R.A.S.-M, T.D.d.P., and R.Z.C.; Formal Analysis, G.L.-T., J.G.-J., R.A.S.-M., T.D.d.P., and R.Z.C.; Data Curation, R.Z.C.; Writing – Original Draft, G.L.T.; Writing – Review and Editing, J.G.-J., R.A.S.-M., T.D.d.P., A.O., and M.C.D.; Resources, T.D.d.P. and A.J.R.H.; Supervision, T.D.d.P.; Project Administration, T.D.d.P.; Funding Acquisition, T.D.d.P.

DECLARATION OF INTERESTS

The authors declare no competing interests.

REFERENCES

1. Blount, Z.D. (2015). The unexhausted potential of *E. coli*. Elife *4*, e058266. https://doi.org/10.7554/eLife.05826.
2. Aebersold, R., and Mann, M. (2016). Mass-spectrometric exploration of proteome structure and function. Nature *537*, 347–355. https://doi.org/10.1038/nature19949.
3. Macek, B., Forchhammer, K., Hardouin, J., Weber-Ban, E., Grangeasse, C., and Mijakovic, I. (2019). Protein post-translational modifications in bacteria. Nat. Rev. Microbiol. *17*, 651–664. https://doi.org/10.1038/s41579-019-0243-0.
4. Christensen, D.G., Baumgartner, J.T., Xie, X., Jew, K.M., Basisty, N., Schilling, B., Kuhn, M.L., and Wolfe, A.J. (2019). Mechanisms, detection, and relevance of protein acetylation in prokaryotes. mBio *10*, e02708-18. https://doi.org/10.1128/mBio.02708-18.
5. Lassak, J., Sieber, A., and Hellwig, M. (2022). Exceptionally versatile take II: post-translational modifications of lysine and their impact on bacterial physiology. Biol. Chem. *403*, 819–858. https://doi.org/10.1515/HSZ-2021-0382.

6. Choudhary, C., Weinert, B.T., Nishida, Y., Verdin, E., and Mann, M. (2014). The growing landscape of lysine acetylation links metabolism and cell signalling. Nat. Rev. Mol. Cell Biol. 15, 536–550. https://doi.org/10.1038/nrm3841.

7. Hentchel, K.L., and Escalante-Semerena, J.C. (2015). Acylation of Biomolecules in Prokaryotes: a Widespread Strategy for the Control of Biological Function and Metabolic Stress. Microbiol. Mol. Biol. Rev. 79, 321–346. https://doi.org/10.1128/mmbr.00020-15.

8. Wolfe, A.J. (2016). Bacterial protein acetylation: new discoveries unanswered questions. Curr. Genet. 62, 335–341. https://doi.org/10.1007/s00294-015-0552-4.

9. Zhao, S., Xu, W., Jiang, W., Yu, W., Lin, Y., Zhang, T., Yao, J., Zhou, L., Zeng, Y., Li, H., et al. (2010). Regulation of Cellular Metabolism by Protein Lysine Acetylation. Science 327, 1000–1004. https://doi.org/10.1126/science.1179689.Regulation.

10. Kuhn, M.L., Zemaitaitis, B., Hu, L.I., Sahu, A., Sorensen, D., Minasov, G., Lima, B.P., Scholle, M., Mrksich, M., Anderson, W.F., et al. (2014). Structural, kinetic and proteomic characterization of acetyl phosphate-dependent bacterial protein acetylation. PLoS One 9, e94816. https://doi.org/10.1371/journal.pone.0094816.

11. Lammers, M. (2021). Post-translational Lysine Ac(et)ylation in Bacteria: A Biochemical, Structural, and Synthetic Biological Perspective. Front. Microbiol. 12, 757179. https://doi.org/10.3389/fmicb.2021.757179.

12. Wang, M.M., You, D., and Ye, B.C. (2017). Site-specific and kinetic characterization of enzymatic and nonenzymatic protein acetylation in bacteria. Sci. Rep. 7, 14790. https://doi.org/10.1038/s41598-017-13897-w.

13. Hosp, F., Lassowskat, I., Santoro, V., De Vleesschauwer, D., Fliegner, D., Redestig, H., Mann, M., Christian, S., Hannah, M.A., and Finkemeier, I. (2017). Lysine acetylation in mitochondria: From inventory to function. Mitochondrion 33, 58–71. https://doi.org/10.1016/j.mito.2016.07.012.

14. Gallego-Jara, J., Ortega, Á., Lozano Terol, G., Sola Martínez, R.A., Cánovas Díaz, M., and de Diego Puente, T. (2021). Bacterial Sirtuins Overview: An Open Niche to Explore. Front. Microbiol. 12, 744416. https://doi.org/10.3389/fmicb.2021.744416.

15. Gallego-Jara, J., Écija Conesa, A., de Diego Puente, T., Lozano Terol, G., and Cánovas Díaz, M. (2017). Characterization of CobB kinetics and inhibition by nicotinamide. PLoS One 12, e0189689. https://doi.org/10.1371/journal.pone.0189689.

16. Weinert, B.T., Iesmantavicius, V., Wagner, S.A., Schölz, C., Gummesson, B., Beli, P., Nyström, T., and Choudhary, C. (2013). Acetyl-Phosphate is a critical determinant of Lysine Acetylation in E.coli. Mol. Cell 51, 265–272. https://doi.org/10.1016/j.molcel.2013.06.003.

17. Schilling, B., Christensen, D., Davis, R., Sahu, A.K., Hu, L.I., Walker-Peddakotla, A., Sorensen, D.J., Zemaitaitis, B., Gibson, B.W., and Wolfe, A.J. (2015). Protein acetylation dynamics in response to carbon overflow in Escherichia coli. Mol. Microbiol. 98, 847–863. https://doi.org/10.1111/mmi.13161.

18. Christensen, D.G., Orr, J.S., Rao, C.V., and Wolfe, A.J. (2017). Increasing Growth Yield and Decreasing Acetylation in Escherichia coli by Optimizing the Carbon-to-Magnesium Ratio in Peptide-Based Media. Appl. Environ. Microbiol. 83, e03034-16.

19. Schilling, B., Basisty, N., Christensen, D.G., Sorensen, D., Orr, J.S., Wolfe, A.J., and Rao, C.V. (2019). Global lysine acetylation in Escherichia coli results from growth conditions that favor acetate fermentation. J. Bacteriol. 201, 1–9. https://doi.org/10.1101/457929.

20. Bernal, V., Castaño-Cerezo, S., and Cánovas, M. (2016). Acetate metabolism regulation in Escherichia coli: carbon overflow, pathogenicity, and beyond. Appl. Microbiol. Biotechnol. 100, 8985–9001. https://doi.org/10.1007/s00253-016-7832-x.

21. Castaño-Cerezo, S., Bernal, V., Post, H., Fuhrer, T., Cappadona, S., Sánchez-Díaz, N.C., Sauer, U., Heck, A.J.R., Altelaar, A.F.M., and Cánovas, M. (2014). Protein acetylation affects acetate metabolism, motility and acid stress response in Escherichia coli. Mol. Syst. Biol. 10, 762–815. https://doi.org/10.15252/msb.20145227.

22. Clomburg, J.M., and Gonzalez, R. (2013). Anaerobic fermentation of glycerol: A platform for renewable fuels and chemicals. Trends Biotechnol. 31, 20–28. https://doi.org/10.1016/j.tibtech.2012.10.006.

23. Li, Z., Nimtz, M., and Rinas, U. (2014). The metabolic potential of Escherichia coli BL21 in defined and rich medium. Microb. Cell Factories 13, 45.

24. Reitzer, L. (2003). Nitrogen Assimilation and Global Regulation in Escherichia coli. Annu. Rev. Microbiol. 57, 155–176. https://doi.org/10.1146/annurev.micro.57.030502.090820.

25. van Heeswijk, W.C., Westerhoff, H.V., and Boogerd, F.C. (2013). Nitrogen Assimilation in Escherichia coli: Putting Molecular Data into a Systems Perspective. Microbiol. Mol. Biol. Rev. 77, 628–695. https://doi.org/10.1128/mmbr.00025-13.

26. Tong, M., French, S., El Zahed, S.S., Ong, W.K., Karp, P.D., and Brown, E.D. (2020). Gene dispensability in Escherichia coli grown in thirty different carbon environments. mBio 11, e02259-20. https://doi.org/10.1128/mBio.02259-20.

27. Xu, J.Y., Xu, Z., Liu, X., Tan, M., and Ye, B.C. (2018). Protein Acetylation and Butyrylation Regulate the Phenotype and Metabolic Shifts of the Endospore-forming Clostridium acetobutylicum. Mol. Cell. Proteomics 17, 1156–1169. https://doi.org/10.1074/mcp.RA117.000372.

28. Carabetta, V.J., Greco, T.M., Tanner, A.W., Cristea, I.M., and Dubnau, D. (2016). Temporal Regulation of the Bacillus subtilis Acetylome and Evidence for a Role of MreB Acetylation in Cell Wall Growth. mSystems 1, e00005-16. https://doi.org/10.1128/msystems.00005-16.

29. Greiner-Haas, F., Bergen, M.v., Sawers, G., Lechner, U., and Türkowsky, D. (2021). Changes of the Proteome and Acetylome during Transition into the Stationary Phase in the Organohalide-Respiring Dehalococcoides mccartyi Strain CBDB1. Microorganisms 9, 365–416. https://doi.org/10.3390/microorganisms9020365.

30. Weinert, B.T., Satpathy, S., Hansen, B.K., Lyon, D., Jensen, L.J., and Choudhary, C. (2017). Accurate quantification of site-specific acetylation stoichiometry reveals the impact of Sirtuin deacetylase CobB on the E. coli acetylome. Mol. Cell. Proteomics 16, 759–769. https://doi.org/10.1074/mcp.M117.067587.

31. Xu, J.-Y., Zhao, L., Xu, Y., Li, B., Zhai, L., Tan, M., and Ye, B.-C. (2020). Dynamic Characterization of Protein and Posttranslational Modification Levels in Mycobacterial Cholesterol Catabolism. mSystems 5, e00424-19. https://doi.org/10.1128/msystems.00424-19.

32. Kosono, S., Tamura, M., Suzuki, S., Kawamura, Y., Yoshida, A., Nishiyama, M., and Yoshida, M. (2015). Changes in the acetylome and succinylome of Bacillus subtilis in response to carbon source. PLoS One 10, e0131169. https://doi.org/10.1371/journal.pone.0131169.

33. Gaviard, C., Broutin, I., Cosette, P., Dé, E., Jouenne, T., and Hardouin, J. (2018). Lysine Succinylation and Acetylation in Pseudomonas aeruginosa. J. Proteome Res. 17, 2449–2459. https://doi.org/10.1021/acs.jproteome.8b00210.

34. Okanishi, H., Kim, K., Masui, R., and Kuramitsu, S. (2013). Acetylome with Structural Mapping Reveals the Significance of Lysine Acetylation in Thermus thermophilus. J. Proteome Res. 12, 3952–3968. https://doi.org/10.1021/pr400245k.

35. Novak, J., Fabrik, I., Jurnecka, D., Holubova, J., Stanek, O., and Sebo, P. (2020). Bordetella pertussis Acetylome is Shaped by Lysine Deacetylase Bkd1. J. Proteome Res. 19, 3680–3696. https://doi.org/10.1021/acs.jproteome.0c00178.

36. Zhang, M., Liu, T., Wang, L., Huang, Y., Fan, R., Ma, K., Kan, Y., Tan, M., and Xu, J.Y. (2023). Global landscape of lysine acylomes in Bacillus subtilis. J. Proteonomics 271, 104767. https://doi.org/10.1016/j.jprot.2022.104767.

37. Jers, C., Ravikumar, V., Lezyk, M., Sultan, A., Sjöling, Å., Wai, S.N., and Mijakovic, I. (2017). The Global Acetylome of the Human Pathogen Vibrio cholerae V52 Reveals Lysine Acetylation of Major Transcriptional Regulators. Front. Cell. Infect. Microbiol. 7, 537–613. https://doi.org/10.3389/fcimb.2017.00537.

38. Yang, H., Sha, W., Liu, Z., Tang, T., Liu, H., Qin, L., Cui, Z., Chen, J., Liu, F., Zheng, R., et al. (2018). Lysine acetylation of DosR regulates the hypoxia response of Mycobacterium tuberculosis. Emerg. Microb. Infect. 7, 1–14. https://doi.org/10.1038/s41426-018-0032-2.

39. Christensen, D.G., Meyer, J.G., Baumgartner, J.T., D'Souza, A.K., Nelson, W.C., Payne, S.H., Kuhn, M.L., Schilling, B., and Wolfe, A.J. (2018). Identification of Novel Protein Lysine Acetyltransferases in Escherichia coli. mBio 9, 1–23. https://doi.org/10.1128/mBio.

40. Schastnaya, E., Doubleday, P.F., Maurer, L., and Sauer, U. (2023). Non-enzymatic acetylation inhibits glycolytic enzymes in Escherichia coli. Cell Rep. 42, 111950. https://doi.org/10.1016/j.celrep.2022.111950.

41. Feid, S.C., Walukiewicz, H.E., Wang, X., Nakayasu, E.S., Rao, C.V., and Wolfe, A.J. (2022). Regulation of Translation by Lysine Acetylation in Escherichia coli. mBio 13, e0122422. https://doi.org/10.1128/mbio.01224-22.

42. Venkat, S., Gregory, C., Sturges, J., Gan, Q., and Fan, C. (2017). Studying the Lysine Acetylation of Malate Dehydrogenase. J. Mol. Biol. 429, 1396–1405. https://doi.org/10.1016/j.jmb.2017.03.027.

43. Bi, J., Wang, Y., Yu, H., Qian, X., Wang, H., Liu, J., and Zhang, X. (2017). Modulation of Central Carbon Metabolism by Acetylation of Isocitrate Lyase in Mycobacterium

tuberculosis. Sci. Rep. *7*, 1–11. https://doi.org/10.1038/srep44826.

44. Görke, B., and Stülke, J. (2008). Carbon catabolite repression in bacteria: Many ways to make the most out of nutrients. Nat. Rev. Microbiol. *6*, 613–624. https://doi.org/10.1038/nrmicro1932.

45. Kremling, A., Geiselmann, J., Ropers, D., and de Jong, H. (2015). Understanding carbon catabolite repression in *Escherichia coli* using quantitative models. Trends Microbiol. *23*, 99–109. https://doi.org/10.1016/j.tim.2014.11.002.

46. Dharmadi, Y., Murarka, A., and Gonzalez, R. (2006). Anaerobic Fermentation of Glycerol by *Escherichia coli*: A New Platform for Metabolic Engineering. Biotechnol. Bioeng. *94*, 821–829. https://doi.org/10.1002/bit.21025.

47. Yu, B.J., Kim, J.A., Moon, J.H., Ryu, S.E., and Pan, J.G. (2008). The diversity of lysine-acetylated proteins in *Escherichia coli*. J. Microbiol. Biotechnol. *18*, 1529–1536. 7509 [pii].

48. Valgepea, K., Adamberg, K., Nahku, R., Lahtvee, P.-J., Arike, L., and Vilu, R. (2010). Systems biology approach reveals that overflow metabolism of acetate in *Escherichia coli* is triggered by carbon catabolite repression of acetyl-CoA synthetase. BMC Syst. Biol. *4*, 166–213. https://doi.org/10.1186/1752-0509-4-166.

49. Bettenbrock, K., Fischer, S., Kremling, A., Jahreis, K., Sauter, T., and Gilles, E.D. (2006). A quantitative approach to catabolite repression in *Escherichia coli*. J. Biol. Chem. *281*, 2578–2584. https://doi.org/10.1074/jbc.M508090200.

50. Perrenoud, A., and Sauer, U. (2005). Impact of global transcriptional regulation by ArcA, ArcB, Cra, Crp, Cya, Fnr, and Mlc on glucose catabolism in *Escherichia coli*. J. Bacteriol. *187*, 3171–3179. https://doi.org/10.1128/JB.187.9.3171-3179.2005.

51. Martínez-Gómez, K., Flores, N., Castañeda, H.M., Martínez-Batallar, G., Hernández-Chávez, G., Ramírez, O.T., Gosset, G., Encarnación, S., and Bolivar, F. (2012). New insights into *Escherichia coli* metabolism: carbon scavenging, acetate metabolism and carbon recycling responses during growth on glycerol. Microb. Cell Factories *11*, 46. https://doi.org/10.1186/1475-2859-11-46.

52. Mori, M., Zhang, Z., Banaei-Esfahani, A., Lalanne, J.B., Okano, H., Collins, B.C., Schmidt, A., Schubert, O.T., Lee, D.S., Li, G.W., et al. (2021). From coarse to fine: the absolute *Escherichia coli* proteome under diverse growth conditions. Mol. Syst. Biol. *17*, 95366. https://doi.org/10.15252/msb.20209536.

53. Baeza, J., Dowell, J.A., Smallegan, M.J., Fan, J., Amador-Noguez, D., Khan, Z., and Denu, J.M. (2014). Stoichiometry of site-specific lysine acetylation in an entire proteome. J. Biol. Chem. *289*, 21326–21338. https://doi.org/10.1074/jbc.M114.581843.

54. Lozano Terol, G., Gallego-Jara, J., Sola Martínez, R.A., Cánovas Díaz, M., and De Diego Puente, T. (2019). Engineering protein production by rationally choosing a carbon and nitrogen source using *E. coli* BL21 acetate metabolism knockout strains. Microb. Cell Factories *18*, 151–219. https://doi.org/10.1186/s12934-019-1202-1.

55. Kheirabadi, E., and Macia, J. (2022). Development and evaluation of culture media based on extracts of the cyanobacterium *Arthrospira platensis*. Front. Microbiol. *13*, 972200. https://doi.org/10.3389/fmicb.2022.972200.

56. Gallego-Jara, J., de Diego, T., Del Real, Á., Écija-Conesa, A., Manjón, A., and Cánovas, M. (2015). Lycopene overproduction and *in situ* extraction in organic-aqueous culture systems using a metabolically engineered *Escherichia coli*. Amb. Express *5*, 65. https://doi.org/10.1186/s13568-015-0150-3.

57. Oestreich, A.M., Suli, M.I., Gerlach, D., Fan, R., and Czermak, P. (2021). Media development and process parameter optimization using statistical experimental designs for the production of nonribosomal peptides in *Escherichia coli*. Electron. J. Biotechnol. *52*, 85–92. https://doi.org/10.1016/j.ejbt.2021.05.001.

58. Fernández-Gutierrez, D., Veillette, M., Ávalos Ramirez, A., Giroir-Fendler, A., Faucheux, N., and Heitz, M. (2020). Biovalorization of glucose in four culture media and effect of the nitrogen source on fermentative alcohols production by *Escherichia coli*. Environ. Technol. *41*, 211–221. https://doi.org/10.1080/09593330.2018.1494751.

59. Liu, Y., Zhang, Z., Jiang, W., and Gu, Y. (2022). Protein acetylation-mediated cross regulation of acetic acid and ethanol synthesis in the gas-fermenting *Clostridium ljungdahlii*. J. Biol. Chem. *298*, 101538. https://doi.org/10.1016/j.jbc.2021.101538.

60. Mizuno, Y., Nagano-Shoji, M., Kubo, S., Kawamura, Y., Yoshida, A., Kawasaki, H., Nishiyama, M., Yoshida, M., and Kosono, S. (2016). Altered acetylation and succinylation profiles in *Corynebacterium glutamicum* in response to conditions inducing glutamate overproduction. Microbiol. *5*, 152–173. https://doi.org/10.1002/mbo3.320.

61. Cox, J., and Mann, M. (2008). MaxQuant enables high peptide identification rates, individualized p.p.b.-range mass accuracies and proteome-wide protein quantification. Nat. Biotechnol. *26*, 1367–1372. https://doi.org/10.1038/nbt.1511.

62. Tyanova, S., Temu, T., Sinitcyn, P., Carlson, A., Hein, M.Y., Geiger, T., Mann, M., and Cox, J. (2016). The Perseus computational platform for comprehensive analysis of (prote)omics data. Nat. Methods *13*, 731–740. https://doi.org/10.1038/nmeth.3901.

63. O'Shea, J.P., Chou, M.F., Quader, S.A., Ryan, J.K., Church, G.M., and Schwartz, D. (2013). PLogo: A probabilistic approach to visualizing sequence motifs. Nat. Methods *10*, 1211–1212. https://doi.org/10.1038/nmeth.2646.

64. Huang, D.W., Sherman, B.T., Tan, Q., Kir, J., Liu, D., Bryant, D., Guo, Y., Stephens, R., Baseler, M.W., Lane, H.C., and Lempicki, R.A. (2007). DAVID Bioinformatics Resources: Expanded annotation database and novel algorithms to better extract biology from large gene lists. Nucleic Acids Res. *35*, 169–175. https://doi.org/10.1093/nar/gkm415.

65. Martinez-Val, A., Garcia, F., Ximénez-Embún, P., Martínez Teresa-Calleja, A., Ibarz, N., Ruppen, I., and Munoz, J. (2017). Urea Artifacts Interfere with Immuno-Purification of Lysine Acetylation. J. Proteome Res. *16*, 1061–1068. https://doi.org/10.1021/acs.jproteome.6b00463.

66. Krstic, J., Reinisch, I., Schindlmaier, K., Galhuber, M., Riahi, Z., Berger, N., Kupper, N., Moyschewitz, E., Auer, M., Michenthaler, H., et al. (2022). Fasting improves therapeutic response in hepatocellular carcinoma through p53-dependent metabolic synergism. Sci. Adv. *8*, eabh2635. https://doi.org/10.1126/sciadv.abh2635.

67. Cox, J., Neuhauser, N., Michalski, A., Scheltema, R.A., Olsen, J.V., and Mann, M. (2011). Andromeda : A Peptide Search Engine Integrated into the MaxQuant Environment. J. Proteome Res. *10*, 1794–1805. https://doi.org/10.1021/pr101065j.

68. Cox, J., Hein, M.Y., Luber, C.A., Paron, I., Nagaraj, N., and Mann, M. (2014). Accurate Proteome-wide Label-free Quantification by Delayed Normalization and Maximal Peptide Ratio Extraction , Termed MaxLFQ. Mol. Cell. Proteomics *13*, 2513–2526. https://doi.org/10.1074/mcp.M113.031591.

69. Schilling, B., Meyer, J.G., Wei, L., Ott, M., and Verdin, E. (2019). High-Resolution Mass Spectrometry to Identify and Quantify Acetylation Protein Targets. In An Automated Irrigation System Using Arduino Microcontroller, pp. 3–16. https://doi.org/10.1007/978-1-4939-9434-2_1.

70. Miller, G.L. (1959). Use of Dinitrosalicylic Acid Reagent for Determination of Reducing Sugar. Anal. Chem. *31*, 426–428.

71. Castaño-Cerezo, S., Renilla, S., Bernal, V., and Cánovas, M. (2009). An insight into the role of phosphotransacetylase (*pta*) and the acetate/acetyl-CoA node in *Escherichia coli*. Microb. Cell Factories *8*, 1–19. https://doi.org/10.1186/1475-2859-8-54.

STAR★METHODS

KEY RESOURCES TABLE

REAGENT or RESOURCE	SOURCE	IDENTIFIER
Antibodies		
PTMScan® Acetyl-Lysine Motif [Ac-K] Kit	Cell Signaling Technology	Cat# 13416S
Bacterial and virus strains		
Escherichia coli BW25113	CGSC	CGSC 7636
Chemicals, peptides, and recombinant proteins		
Sodium Deoxycholate (SDC)	Thermo Fisher Scientific	Cat# 89904
Trypsin Gold, Mass Spectrometry Grade	Promega	Cat# V528A
3,5-Dinitrosalicylic acid (DNS)	Sigma	Cat# 128848
Phenylhydrazine	Sigma	Cat# P26252
DL-Isocitric acid, trisodium salt hydrate, 95%	Thermo Fisher Scientific	Cat# 10053573
DL-Glyceraldehyde 3-phosphate solution	Sigma	Cat# G5251
HEPES buffer	Thermo Fisher Scientific	Cat# 11412497
NAD^+, Lithium Salt	Sigma	Cat# 481915
Magnesium chloride hexahydrate	Thermo Fisher Scientific	Cat# 15607980
DL-Malic acid	Sigma	Cat# 240176
Critical commercial assays		
Pierce™ Quantitative Colorimetric Peptide Assay kit	Thermo Fisher Scientific	Cat# 23275
Deposited data		
Raw proteomics data	This study	PRIDE: PXD041209 (https://www.ebi.ac.uk/pride/archive/)
Software and algorithms		
MaxQuant (version 2.0.3.1)	Cox and Mann et al.[61]	https://www.maxquant.org/
Perseus (version 1.6.15.0)	Tyanova et al.[62]	https://maxquant.net/perseus/
pLogo	O'Shea et al.[63]	https://plogo.uconn.edu/
DAVID database (Database for Annotation, Visualisation and Integrated Discovery)	Huang et al.[64]	https://david.ncifcrf.gov/

RESOURCE AVAILABILITY

Lead contact

Further information and requests for resources and reagents should be directed to and will be fulfilled by the lead contact, Prof. Dr. Teresa de Diego Puente (tdp@um.es).

Materials availability

This study did not generate new unique reagents.

Data and code availability

- The raw mass spectrometry proteomics data generated in this study have been deposited in the ProteomeXchange Consortium via the PRIDE partner repository with the dataset identifier PXD041209 and are publicly available as of the date of publication. Accession numbers are listed in the key resources table.
- This paper does not report original code.
- Any additional information required to reanalyze the data reported in this paper is available from the lead contact upon request.

EXPERIMENTAL MODEL AND STUDY PARTICIPANT DETAILS

Experiments were carried out in *E. coli* BW25113 strain obtained from the Coli Genetic Stock Center (CGSC) (strain 7636). *E. coli* was grown using M9 minimal medium or TB7 complex medium, supplemented with glucose (20 mM) or glycerol (40 mM) as carbon source Cultures were incubated at 37°C under constant shaking at 200 rpm.

METHOD DETAILS

Cell cultures and acetylated peptide enrichment

E. coli K12 BW25113 strain was grown employing TB7 complex medium (10 g/L tryptone buffered at pH 7.0 with 100 mM potassium phosphate) or M9 minimal medium (10 mM $(NH_4)_2SO_4$, 8.5 mM NaCl, 40 mM Na_2HPO_4, 20 mM KH_2PO_4, 185 μM $FeCl_3$, 175 μM EDTA, 7 μM $ZnSO_4$, 7 μM $CuSO_4 \cdot 5\ H_2O$, 7 μM $MnSO_4$, 7 μM $CoCl_2$, 1 mM $MgSO_4$, 0.1 mM $CaCl_2$, and 1 μM thiamine HCl), supplemented with glucose 20 mM or glycerol 40 mM as carbon source. Therefore, 4 culture conditions (TB7-glucose, TB7-glycerol, MM9-glucose, and MM9-glycerol) were used. Cultures were inoculated at an initial optical density (OD_{600}) of 0.05 units with exponentially growing precultures, and samples were taken in exponential and in stationary growth phase (Figure S5), resulting in 8 experimental samples: TB7-glucose in exponential phase, TB7-glucose in stationary phase, TB7-glycerol in exponential phase, TB7-glycerol in stationary phase, MM9-glucose in exponential phase, MM9-glucose in stationary phase, MM9-glycerol in exponential phase, and MM9-glycerol in stationary phase, with 4 biological replicates from each. Cells were harvested by centrifugation at 2000 x g for 30 min at 4°C, cell pellets were washed with PBS buffer twice, and preserved at -80°C until cell lysis.

Cell pellets were resuspended in lysis buffer containing 4% sodium deoxycholate (SDC) in 100 mM Tris-HCl buffer at pH 8.5.[65] Samples were incubated with lysis buffer at 99°C for 10 min with shaking, then cooled to room temperature for 15 min and sonicated for 2 min and 30s (cycles of 10 sec each) using the Vibra Cell sonicator (Sonicator Sonics & Materials). Lysates were clarified at 12000 x g for 30 min at 4°C, and 1.5 mg of proteins were taken from each sample for proteolysis. Proteins were reduced by addition of 10 mM DTT for 1 h at 37°C and alkylated by incubation with 25 mM iodoacetamide for 30 min in the dark at room temperature. Samples were digested with Trypsin Gold (Promega) at a 1/50 (w/w) trypsin/protein ratio for 16 h at 37°C. Samples were acidified by addition of formic acid and desalted using Sep-Pak C18 3 cc Vac Cartridge columns (Waters). Tryptic peptides were dried by vacuum centrifugation at 4°C.

Tryptic peptides were resuspended in immunoaffinity buffer (50 mM MOPS, 10 mM Na_2HPO_4, 50 mM NaCl, pH 7.2) and their concentration was measured using the Pierce™ Quantitative Colorimetric Peptide Assay kit (Thermo Fisher Scientific). An aliquot of 50 μg of each sample was isolated for proteome quantitative analysis. The remaining tryptic peptide samples were employed for enrichment and purification of acetylated peptides using an antiacetyllysine antibody-bead conjugate. Thus, 1 mg of peptides from each sample was taken and incubated with 1/4 of a tube of the PTMScan acetyllysine motif [Ac-K] kit (Cell Signaling Technologies) for 2 h at 4°C in rotation, according to the manufacturer's instructions. After incubation with the antibodies, samples enriched in acetylated peptides were desalted and concentrated using the Oasis HLB 96-well μElution Plate, and subsequently dried by vacuum centrifugation at 4°C.

LC-MS parameters

Proteome and acetylome samples were analyzed using an Ultimate3000 high-performance liquid chromatography system (Thermo Fisher Scientific) coupled online to a Orbitrap Exploris 480 mass spectrometer (Thermo Fisher Scientific) as previously described[66] with minor modifications. Buffer A consisted of water acidified with 0.1% formic acid, while buffer B was 80% acetonitrile and 20% water with 0.1% formic acid. The peptides were first trapped for 1 min at 30 μL/min with 100% buffer A on a trap (0.3 mm by 5 mm with PepMap C18, 5 μm, 100 Å; Thermo Fisher Scientific); after trapping, the peptides were separated by a 50 cm analytical column packed with C18 beads (Poroshell 120 EC-C18, 2.7 μm; Agilent Technologies). The gradient was 9 to 40% B in 40 min at 300 nL/min. Buffer B was then raised to 55% in 5 min and finally increased to 99% for the cleaning step. Peptides were ionized using a spray voltage of 2 kV and a capillary heated at 275°C. The mass spectrometer was set to acquire full-scan MS spectra (350 to 1400 mass/charge ratio) for a maximum injection time of 120 ms at a mass resolution of 120000 and an automated gain control (AGC) target value of 3×10^6. The most intense precursor ions were selected for MS/MS in a full cycle of 1 second (data-dependent acquisition, DDA). In both type of samples, we used HCD fragmentation in the HCD cell, with the readout in the Orbitrap mass analyser; for the full proteome we used a resolution of 15000 (isolation window of 2.4 Th), while for the acetylated peptides only we used a resolution of 30000 to have highest possible quality of modified spectra. All the other parameters were the same: the AGC target value was set to 1×10^5 with a maximum injection time "Auto" and a normalized collision energy of 28%.

Data analysis

Raw data files from proteome and acetylome were processed with MaxQuant software (version 2.0.3.1) integrated with the Andromeda search system.[67] Data were searched against the Uniprot database of the *E. coli* K12 reference proteome (December 2021; 4448 sequences), also allowing the identification of contaminants. Identification of acetylated sites was performed using the following set of parameters in MaxQuant. Trypsin was chosen as cleavage specificity, allowing a maximum of three missed cleavages. Carbamidomethylation (C) was selected as a fixed modification, and oxidation (M), acetylation (N-terminal), deamidation (N and Q), and lysine acetylation (K) were selected as variable modifications, with a maximum number of modifications per peptide being 5. The minimum length of each peptide was set to 6 amino acids and the maximum mass to 5600 Da. Database searches were performed by setting peptide mass tolerance to 20 ppm for the first search and 4.5 ppm for the main search. Mass tolerance for fragments ions from HCD was 20 ppm. For data filtering, the minimum Andromeda

score for modified peptides was set to 40, the minimum delta score for modified peptides was set to 6, and the false discovery rate (FDR) for peptide, protein, and modification site identification was set at 1%. Parameters used to process proteome data were identical to those shown, except for the removal of lysine acetylation as a variable modification and the allowance of 2 missed cleavages. Proteins were quantified employing the MaxLFQ function of MaxQuant,[68] using only unmodified peptides and those showing oxidation (M) and acetylation (N-term), with at least two identifications of each peptide required for pairwise comparisons of abundance between samples.

Student's t-tests (s0= 0.1; FDR based on permutations ≤ 0.05) were performed using Perseus software (version 1.6.15.0) to relatively quantify changes in protein abundance and acetylation level between culture conditions. Student's t-tests were performed with peptides or proteins present in the two samples to be compared in at least 3 of the 4 biological replicates. Prior to performing statistical tests, contaminants and reverse sequences were removed, and data were log-transformed. Furthermore, in acetylome samples, only acetylation sites with a localisation probability greater than 0.75 were used for further analysis, and intensity values of peptides were normalised. For normalisation, intensity values of acetylated peptides were relativised to intensity values of proteins to which they belong in each sample.[69] The general workflow, from culture to sample analysis, is shown in Figure S8.

pLogo software[63] was used for consensus acetylation motif analysis, selecting 15 residues surrounding each side of acetylated lysine. Functional annotation and enrichment was performed by analysis of GO (Gene Ontology) terms using DAVID database (Database for Annotation, Visualisation and Integrated Discovery; version v2022q1).[64] Benjamini-Hochberg correction was used for p-value adjustment, and a p-value < 0.05 was set as the threshold for statistical significance in enrichment analysis on selected GO terms.

Cell growth and acetate concentration analysis

E. coli K12 BW25113 strain was grown on TB7 complex medium or M9 minimal medium, supplemented with glucose (20 mM) or glycerol (40 mM) as carbon source. Cultures were inoculated at an initial OD_{600} of 0.05 with exponentially growing precultures, and specific growth rate was determined.[51] To quantify extracellular acetate concentration, 1 mL of sample was taken from cultures at different growth times and centrifuged at 12000 x g for 1 min at 4°C. The supernatant was preserved at -20°C until analysis. An HPLC equipped with a differential refractometer and UV detectors (Shimadzu Scientific Instruments) with an ion-exclusion column (ICSep Coregel 87H3, Transgenomic) was used to analyse extracellular acetate concentration. The mobile phase was 5 mM H_2SO_4 flowing at 0.5 mL min^{-1} and 65°C. Glucose consumption was determined by the dinitrosalicylic acid (DNS) method.[70]

Enzymatic assay

Glyceraldehyde-3-phosphate dehydrogenase, malate dehydrogenase, and isocitrate lyase activity were assayed as previously described.[40,71] *E. coli* K12 BW25113 strain was grown in duplicate on M9 minimal medium or TB7 complex medium, supplemented with glucose (20 mM) or glycerol (40 mM) as carbon source, and samples were taken in exponential and in stationary growth phase (Figure S5). Cells were separated by centrifugation at 4500 rpm for 10 min at 4°C and resuspended in 65 mM phosphate buffer pH 7.5. Cells were disrupted on ice by sonication for 1 min (cycles of 10 sec each) using the Vibra Cell sonicator (Sonicator Sonics & Materials). The cell extract was centrifuged for 20 min at 12000 rpm and 4°C, and the supernatant was preserved for enzymatic assays. Protein concentration was measured and an equal amount of total proteins was employed in all assays. Enzymatic activity in each sample was relativised to the intensity values of GapA, Mdh, and AceA proteins in each sample.

The glyceraldehyde-3-phosphate dehydrogenase activity was performed in 10 mM Na_2HPO_4 and 100 mM HEPES buffer pH 7.2, with 2 mM glyceraldehyde 3-phosphate and 1 mM NAD^+, and the reaction was followed by the increase in NADH absorbance at 340 nm (6220 $M^{-1}cm^{-1}$). Malate dehydrogenase activity was conducted in 100 mM HEPES buffer pH 7.2, with the addition of 10 mM $MgCl_2$, 5 mM malate, and 1 mM NAD^+. The reaction was monitored by the increase in absorbance at 340 nm (6220 $M^{-1}cm^{-1}$). To measure isocitrate lyase activity the assays were performed in 65 mM phosphate buffer pH 7.5, with the addition of 20 mM phenylhydrazine, 5 mM $MgCl_2$, and 5 mM D, L-sodium isocitrate. The reaction was followed by the increase in absorbance at 324 nm due to the reaction of the phenylhydrazine with the glyoxylate produced (16.8 $M^{-1}cm^{-1}$). One unit of activity was defined as the amount of enzyme needed to convert 1 μmol of sustrate per minute.

QUANTIFICATION AND STATISTICAL ANALYSIS

Details for specific statistical tests and replicates can be found in the figure legends and method details section.